Uncertainty quantification for random Hamiltonian systems by using polynomial expansions and geometric integrators

Marc Jornet

Departament de Matemàtiques,
Universitat Jaume I,
12071 Castellón, Spain.
email: jornet@uji.es

Abstract. Recent advances in the field of uncertainty quantification are based on achieving suitable functional representations of the solutions to random systems. This aims at improving the performance of Monte Carlo simulation, at least for low-dimensional problems and moderately large independent variable. One of these functional representations are the so-called generalized polynomial chaos (gPC) expansions, based upon orthogonal polynomial decompositions. When the input random parameters are independent (a germ), a Galerkin projection technique applied to the truncated gPC expansion is usually employed. This approach exhibits fast mean-square convergence for smooth dynamics, whenever applicable. However, the main difficulty arises when solving the Galerkin system for the gPC coefficients, which may rely on different solvers (algorithms and codes) than those for the original system. A recent contribution noticed that, for random Hamiltonian systems, the Galerkin system is Hamiltonian too. Thus, the well-known symplectic integrators can be applied. The present paper investigates random Hamiltonian systems in general, when the input random parameters may be non-independent. In such a case, polynomial expansions based on the canonical basis and an imitation of the Galerkin projection technique are proposed. The Hamiltonian structure of the original system is unfortunately not conserved, but volume preservation is. Hence volume-preserving integrators are of use. Numerical experiments suggest that the proposed polynomial expansions may be useful for fast and accurate uncertainty quantification.

Keywords: random Hamiltonian system; non-independent input parameters; uncertainty quantification; intrusive polynomial expansion; canonical polynomial basis; volume-preserving integrator

AMS Classification 2010: 34F05; 37J05; 65C30; 65L05

1. Introduction

For physical systems formulated by mathematical models (ordinary and partial differential equations), simulations are necessary to predict the behavior of the system. For that purpose, extensive efforts have been devoted to the development of efficient numerical integrators [1–4]. However, for a proper description of the true physics, uncertain errors should be taken into account. By uncertain errors, it is understood the inherent errors of the collected data, due to limitations of the experiments, bad measurements, incomplete knowledge of the system, etc. [5, Chapter 1]. Uncertain errors are distinct to numerical errors, which are under control in general.

Data errors confer variability on the model parameters. Indeed, parameters are set from data, empirically or by least-squares optimization procedures. Such variability is treated mathematically within a probabilistic framework. The parameters are assumed to be random

variables, and the model output becomes a random process. A single numerical simulation, for a particular parameter value, is not enough to predict the process. Rather, its statistical content (mean, variance, probability density) is the main interest. The field of uncertainty quantification, as the name implies, is devoted to the investigation of models for which uncertain data errors are not neglected, and to quantify the impact of such errors on parameters (inverse problem) and on outputs (forward problem) [5–7].

Numerical methods for random systems are not a simple extension of the deterministic (i.e. non-random) counterpart. The classical approach for (forward) uncertainty quantification is based on Monte Carlo simulation [8, 9]. By the law of large numbers, it estimates any quantity that involves an element of randomness by sampling. The method is easy to implement and robust: the procedure and the convergence rate are independent of the model, of the smoothness, of the parameter dimension, of the time variable, etc. However, the root-mean-square error for the mean value decays as the reciprocal of the square root of the sample length (by the central limit theorem). This may be slow, especially when a realization of the model output is time-consuming or high precision in the statistics estimates is sought. The intuition for this slowness is the following: a realization only provides local information, which penalizes the problem of determining the global variability [6, Chapter 1]. Thus, research has been devoted to reconstructing the functional dependence of the model output on the parameters (non-statistical methods). Essentially, building a surrogate for the input-output relation. Generalized polynomial chaos (gPC) expansions, developed at the beginning of this century [10] to extend Gaussian-based polynomial chaos (PC) expansions (Hermite chaos, also called Wiener chaos) [11], write the model output in terms of orthogonal polynomials evaluated at the parameters, when the parameters are independent random variables. Those orthogonal polynomials are taken from the Askey-Wiener scheme, Gram-Schmidt procedures and tensor products. Mean-square convergence holds in most cases, at spectral convergence rate (exponential for smooth dynamics), though it gets severely affected by large time variable and high parameter dimension [5, 12–14]. For moderately large time variable and low-dimensional uncertainties, gPC may be highly superior to Monte Carlo. (For large time variable or high random dimension, the Monte Carlo method remains unbeatable.) Many approaches exist for estimating the gPC coefficients: intrusive (Galerkin projection technique [10]), which may need other algorithms and codes compared to the governing model, and non-intrusive (quadratures, least-squares, interpolation... [15]), which employ the same solver as the original model but repeatedly executed. Albeit the Galerkin approach is optimal theoretically, in the sense that the residue of the random governing equations is orthogonal to the linear space spanned by the gPC basis, a variant may be more efficient than another depending on the problem under study [5, pages 87–88], [16].

The Galerkin projection technique constructs an associated Galerkin system for the gPC coefficients. This system is larger than the original one, which may pose serious difficulties in practice. However, when the Galerkin system can be efficiently solved, such intrusive variant offers optimal approximations. In [17], the authors investigated the applicability of the Galerkin projection technique in the setting of random Hamiltonian systems. As they proved, the dynamics of the Galerkin system are also Hamiltonian. This is a very important feature. The well-known symplectic integrators for Hamiltonian dynamics [4, 18] can be applied to these Galerkin systems, which are then solved efficiently, thus yielding optimality of the polynomial representations.

As already mentioned, gPC expansions are employed for independent input parameters. Non-independent parameters are often disregarded in the literature [5, Chapter 4]. (The term "dependent" is not used here as an antonym of "independent" and a synonym of "non-independent", since "dependent" may suggest an explicit functional relationship, which is not the probabilistic concept of non-independence.) This motivates the development of methods for non-independent parameters. Expansions in terms of the canonical polynomial basis (no orthogonal polynomials), by mimicking the Galerkin approach, have been recently investigated [19–21]. Uncertainty quantification can be efficiently conducted in general, without relying on Gram-Schmidt constructions. Further, for independent parameters, the new expansions coincide with Galerkin-based gPC expansions. Nonetheless, a drawback of expanding with respect to the canonical polynomial basis is that the associated Gram matrix is not the identity, in contrast to orthogonal bases. The Gram matrix may be highly ill-conditioned [22]. (The Hilbert matrix arises as the Gram matrix of the canonical basis for the Uniform distribution, for instance.) This may pose serious difficulties. But, in general, small orders of the expansions afford good approximations, and for these small orders the Gram matrix is not excessively ill-conditioned yet.

In the present paper, these polynomial expansions described, which work under non-independence, are investigated in the context of random Hamiltonian systems. An associated Galerkin system is obtained for the expansion coefficients. Unfortunately it is not Hamiltonian, but it is divergence free and hence volume preserving. (Actually, volume refers to oriented volume, which means that the determinant of the Jacobian matrix of the flow is $+1$.) Thus, the result from [17] is extended. This associated system can be solved by relying on volume-preserving integrators [4,23]. As will be seen, some traditional symplectic integrators can be taken as volume preserving for this particular system. Therefore, the distinctive geometric structure gives strength to intrusive variants.

The investigation is organized as follows. In Section 2, the main concepts and notations regarding Hamiltonian systems are given. First, deterministic Hamiltonian systems and their own geometric structure are exposed [4]. Second, the randomization of the Hamiltonian system is conducted [5]. And third, the classical case in which the source of randomness is due to the initial positions and momenta is described [24], to afford the intuition about the importance of the geometric properties of Hamiltonian dynamics on uncertainty quantification. In Section 3, the application of Galerkin-based gPC expansions to random Hamiltonian systems, as well as the preservation of the Hamiltonian structure by the Galerkin system, are reviewed [17]. From these ideas, Section 4 adapts the Galerkin approach to the case of non-independent inputs. Polynomial expansions with respect to the canonical basis, instead of orthogonal families, are utilized. These expansions maintain the divergence-free and, if even with respect to momenta, reversibility structure for the new system of the coefficients, which in addition possesses a first integral (a constant of motion). These new results generalize [17]. Convergence (by extending [20, 21]) and numerical aspects are discussed in detail. Section 5 performs some numerical experiments for prototypical models: harmonic oscillator, undamped and unforced Duffing oscillator, and simple gravity pendulum. Some input parameters are assumed to have probability distributions, and the mean, the standard deviation and the probability density of the response are approximated. The system of the expansion coefficients is solved by the Störmer-Verlet integrator, which is volume preserving, symmetric and reversible. Finally, Section 6 renders the conclusions.

2. Hamiltonian systems and their randomization

2.1. **A brief glance into (deterministic) Hamiltonian systems.** The state space of a system is represented by the coordinates $q = (q_1, \ldots, q_n)^\top$ and the momenta $p = (p_1, \ldots, p_n)^\top$. From Newton's second law, the equations of motion are

$$\dot{q}_i = \frac{\partial H}{\partial p_i}, \quad \dot{p}_i = -\frac{\partial H}{\partial q_i}, \quad i = 1, \ldots, n, \tag{2.1}$$

where $H(q, p)$ is the Hamiltonian function. This is a Hamiltonian system. Its flow $\varphi_t(x)$, $x = (q, p)$, has important geometric features: symplecticity and reversibility. The flow is symplectic if its Jacobian matrix $\varphi_t'(x)$ verifies

$$\varphi_t'(x)^\top J \varphi_t'(x) = J, \quad t \geq 0, \tag{2.2}$$

where

$$J = \begin{pmatrix} O_n & I_n \\ -I_n & O_n \end{pmatrix}$$

is the basic canonical matrix, I_n is the $n \times n$ identity matrix, and O_n is the $n \times n$ zero matrix. This identity implies that the flow preserves (oriented) volume in phase space,

$$\text{volume of } \varphi_t(D) = \text{volume of } D.$$

That is, $\det(\varphi_t'(x)) = 1$. Symplecticity characterizes the property of a differential system of being Hamiltonian. When $n = 1$, symplecticity is equivalent to preservation of volume (area). On the other hand, reversibility of a map means that

$$\varphi_t \circ S \circ \varphi_t = S,$$

where $\circ$ denotes composition and S is the momentum flip map $S(q, p) = S(q, -p)$. For Hamiltonian systems, the flow is reversible if and only if the Hamiltonian H is an even function of p.

The dynamics associated to Hamiltonian systems are thus restrictive. When numerical simulations are carried out, integrators should obey at the discrete level the symplectic character of the flow. This is the case of semi-implicit Euler's methods (order one), Störmer-Verlet/leapfrog schemes (order two), etc. These two methods are explicit for separable Hamiltonians, i.e. those that decompose into kinetic energy and potential energy: $H(q, p) = \frac{1}{2} p^\top M^{-1} p + V(q)$, where M is a positive definite mass matrix. In the field of geometric numerical integration, efforts are on reproducing geometric features of the governing model, rather than on mere consistency and stability. Improvements over classical, non-symplectic methods, such as Euler's (order one), Heun's (order two), etc. rules, are achieved, in terms of error decay, robustness, qualitative behavior and long-term integration [4, 18].

2.2. **Randomization of the Hamiltonian system.** Uncertainty is inherent to the modeling of physical systems. Data errors arise because of limitations of the experiments, incomplete knowledge of the system, etc. Such data variability should be reflected in the mathematical model. Models depend on parameters, which measure physical quantities and are set from data (empirically or by least-squares optimization). Thus, data uncertainty is transmitted to the parameters. The goal of uncertainty quantification is to investigate the impact of data errors on the model output, by randomizing the model parameters from the beginning of the simulations. In this manner, more faithful descriptions and predictions of the true physics are expected [5, 6].

System (2.1) is assumed to depend on a set of parameters $\lambda = (\lambda_1, \ldots, \lambda_d)^\top$. These parameters may belong to the equations, the initial conditions, the boundary values, or even the region of definition of the problem. Further, $\lambda = \lambda(\theta)$ is considered as a random vector, on a complete probability space $(\Theta, \mathscr{F}, \mathbb{P})$ with elementary outcomes $\theta \in \Theta$. Under this framework, the coordinates $q = q(t;\lambda)$ and the momenta $p = p(t;\lambda)$ are random processes, which solve the governing system (2.1) for each λ in a smooth, classical way (sample-path, or pathwise, solution [25]). (Itô's equations, driven by irregular white noise, are not treated here [7, pages 96–98], [26–28].) The objective of uncertainty quantification is the following: Given a probability law for λ, which are the distributions of $q(t;\lambda)$ and $p(t;\lambda)$? Actually, the distribution of a random process is the set of all finite-dimensional distributions. In practice, only part of the statistical content of the process is extracted, namely the mean, the variance, or the probability density if possible.

Really, what is referred to as uncertainty quantification in this work is, more precisely, forward uncertainty quantification. Inverse uncertainty quantification consists in inferring the probability distribution of λ from gathered data. This is normally done by means of Bayesian inference [7]. Inverse estimation will not be the subject of the present work; only some comments will be made in the last section.

2.3. **Deterministic Hamiltonian motion subject to random initial conditions.** After randomization of the Hamiltonian dynamics, a first question that naturally arises is whether the geometric structure of the deterministic system has any impact on the random counterpart. Let us focus in this section on a deterministic motion, but subject to random initial states $q_0(\lambda) = q(0;\lambda)$ and $p_0(\lambda) = p(0;\lambda)$. This is the simplest passage from deterministic to random equations [24]. The coordinates and momenta can be written as $q(t;\lambda) = \varphi_t^1(q_0(\lambda), p_0(\lambda))$ and $p(t;\lambda) = \varphi_t^2(q_0(\lambda), p_0(\lambda))$, where $\varphi_t = (\varphi_t^1, \varphi_t^2)$ is the deterministic flow. Since $\varphi_t(\cdot,\cdot)$ is injective and continuously differentiable, with non-vanishing Jacobian $\det(\varphi_t')$, the identity

$$f_{q(t;\lambda),p(t;\lambda)}(q,p) = f_{q_0(\lambda),p_0(\lambda)}(\varphi_t^{-1}(q,p))|\det(\varphi_t'(q,p))^{-1}|$$

holds, where f denotes the corresponding probability density. As the flow is volume preserving, the identity becomes

$$f_{q(t;\lambda),p(t;\lambda)}(q,p) = f_{q_0(\lambda),p_0(\lambda)}(\varphi_t^{-1}(q,p)).$$

This formula is solely verified when the flow preserves volume.

Thus, the geometric properties of the deterministic Hamiltonian dynamics have an effect on the random scenario, and they should have an impact on the development of strategies for uncertainty quantification. From now on, the intention is to study this effect more, when the governing Hamiltonian model possesses any degree of randomness. The so-called gPC expansions, and the projections constructed from them by the Galerkin technique, are greatly influenced by the Hamiltonian character of the model.

3. gPC expansions

The paper [17] already investigated the applicability of gPC expansions for random Hamiltonian systems, so a brief review is simply offered here. It is the hope to enlighten our posterior proposal for uncertainty quantification.

The assumption needed by gPC expansions [5] is the mean-square integrability of the process. That is,

$$q(t;\lambda) \in \mathrm{L}^2(\Theta, \mathrm{d}\mathbb{P}), \quad p(t;\lambda) \in \mathrm{L}^2(\Theta, \mathrm{d}\mathbb{P}), \quad t \geq 0.$$

This simply expresses the existence of finite expectation and variance, two measures that are required for any statistical analysis. A gPC basis is a family of orthogonal polynomials $\{\phi_k(\lambda)\}_{k=1}^{\infty}$:

$$\langle \phi_k(\lambda)\phi_j(\lambda)\rangle = \int_{\mathbb{R}^d} \phi_k(\lambda)\phi_j(\lambda) f_\lambda(\lambda)\,\mathrm{d}\lambda = \begin{cases} 0, & k \neq j, \\ 1, & k = j. \end{cases}$$

This inner product is defined in $\mathrm{L}^2(\Theta, \mathrm{d}\mathbb{P})$, or equivalently in the weighted space $\mathrm{L}^2_{f_\lambda}(\mathbb{R}^d)$. By convention, $\phi_1(\lambda) = 1$. For degree of randomness d equal to 1, this family is usually readily available. If λ belong to the Askey-Wiener scheme, then the family is well-known by recursion and closed-form formulas. For example, the Normal distribution is associated to the Hermite family, the Uniform distribution corresponds to the Legendre family, the Gamma distribution is linked to the Laguerre family, etc. If λ does not dispose of a closed-form family of orthogonal polynomials, a Gram-Schmidt orthogonalization procedure is carried out [29]. For degree of randomness d higher than 1, the family is constructed by tensor products of the univariate families. For such a tensor construction, independence of $\lambda_1, \ldots, \lambda_d$ is crucial. The gPC expansion is

$$q_i(t;\lambda) = \sum_{k=1}^{\infty} Q_{ik}(t)\phi_k(\lambda), \quad p_i(t;\lambda) = \sum_{k=1}^{\infty} P_{ik}(t)\phi_k(\lambda),$$

in the sense of $\mathrm{L}^2(\Theta, \mathrm{d}\mathbb{P})$. The coefficients are deterministic, given by

$$Q_{ik}(t) = \langle q_i(t;\lambda)\phi_k(\lambda)\rangle, \quad P_{ik}(t) = \langle p_i(t;\lambda)\phi_k(\lambda)\rangle. \tag{3.1}$$

Mean-square convergence of the gPC expansion holds whenever the moment problem for $\lambda_1, \ldots, \lambda_d$ is uniquely solvable [12], as a generalization of the Cameron-Martin theorem for Hermite chaos (PC) expansions [30]. (This includes bounded random variables, and more generally random variables with finite moment-generating function; the Lognormal distribution, for instance, fails to satisfy determinacy by its moments.) The rate of mean-square convergence is spectral [5]. (It depends on the smoothness of q_i and p_i with respect to λ, being exponential for analytic dependence, algebraic for C^r dependence, and sublinear for mere continuous dependence.) Nonetheless, it is not uniform with t nor the number of parameters d; it suffers for large t or d [13, 14]. Convergence beyond mean-square is not expected, in general [31].

In practice, the gPC coefficients (3.1) cannot be computed exactly. It is possible to apply quadrature rules, but the governing system needs to be solved for each quadrature node [15]. Another option relies on the Galerkin projection technique [10]. The gPC expansions are truncated,

$$q_i^K(t;\lambda) = \sum_{k=1}^{K} Q_{ik}(t)\phi_k(\lambda), \quad p_i^K(t;\lambda) = \sum_{k=1}^{K} P_{ik}(t)\phi_k(\lambda), \tag{3.2}$$

so that $K = (\deg + d)!/(\deg! d!)$, where deg is the maximum degree of $\{\phi_k(\lambda)\}_{k=1}^K$, $\deg \in \{1, 2, 3, \ldots\}$. The coefficients of (3.2) will differ from (3.1), but will resemble them as K

grows. These coefficients (dependent on K) are obtained by imposing (3.2) to be a solution to (2.1), and afterward applying inner products:

$$\dot{Q}_{ij}(t) = \langle \frac{\partial H}{\partial p_i}(q^K(t;\lambda), p^K(t;\lambda);\lambda)\phi_j(\lambda)\rangle, \tag{3.3}$$

$$\dot{P}_{ij}(t) = \langle -\frac{\partial H}{\partial q_i}(q^K(t;\lambda), p^K(t;\lambda);\lambda)\phi_j(\lambda)\rangle, \quad i = 1,\dots,n, \quad j = 1,\dots,K. \tag{3.4}$$

Here $q^K = (q_1^K,\dots,q_n^K)^\top$ and $p^K = (p_1^K,\dots,p_n^K)^\top$. This is the Galerkin system, of dimension nK (K times larger than the governing system (2.1)). In general, new algorithms and codes are necessitated to solve it. But if an efficient integrator is available for the Galerkin system, then with a single resolution of it, functional representations of $q(t;\lambda)$ and $p(t;\lambda)$ are obtained by the Galerkin projections (3.2). Further, the Galerkin approach is optimal theoretically, in the sense that the residue of the random governing equations is orthogonal to the linear space spanned by the gPC basis. The mean and the standard deviation (σ) are estimated as follows:

$$\langle q_i(t;\lambda)\rangle \approx \langle q_i^K(t;\lambda)\rangle = Q_{i1}(t), \tag{3.5}$$

$$\sigma[q_i(t;\lambda)] \approx \sigma[q_i^K(t;\lambda)] = \sqrt{\sum_{k=2}^{K}(Q_{ik}(t))^2}. \tag{3.6}$$

(The analogous formulas hold for the momenta.) Other statistics, or the probability density, can be estimated by a simple post-processing of the Galerkin projection; only polynomial evaluations at realizations are required.

It turns out that, for Hamiltonian systems, the Galerkin system (3.3)–(3.4) is Hamiltonian too [17]. A new Hamiltonian is defined by averaging H:

$$\hat{H}(Q,P) = \langle H(\left(\sum_{k=1}^{K} Q_{ik}\phi_k(\lambda)\right)_{i=1}^{n}, \left(\sum_{k=1}^{K} P_{ik}\phi_k(\lambda)\right)_{i=1}^{n};\lambda)\rangle,$$
$$Q = (Q_{ik})_{i,k}, \quad P = (P_{ik})_{i,k}.$$

Then (3.3)–(3.4) is equivalent to

$$\dot{Q}_{ij} = \frac{\partial \hat{H}}{\partial P_{ij}}, \quad \dot{P}_{ij} = -\frac{\partial \hat{H}}{\partial Q_{ij}}, \quad i = 1,\dots,n, \quad j = 1,\dots,K. \tag{3.7}$$

Therefore, symplectic integrators can be applied to solve (3.7). These integrators are well-known [4], hence no new algorithms nor codes are necessary. This is, certainly, a very important feature that is not encountered in general systems.

In general, the mean-square convergence of Galerkin projections is not easy to establish from the convergence of gPC expansions (despite the convergence of orthogonal expansions being a classical topic [32, 33]). The reference [34] proves convergence of the Galerkin projection when the associated gPC expansion converges at least exponentially and the vector field of the governing system meets a global Lipschitz condition. This condition is quite restrictive, but common when dealing with mean-square limits in random differential equation problems [35, Theorem 5 and subsequent example]. In any case, in numerical experiments it is usually observed spectral convergence rate, as earlier described for the gPC expansions. Thus, an efficient alternative to Monte Carlo simulation is available, at least for low dimension d and moderate t.

Recall that this approach, as already stated, presumes that the input random parameters are independent. Most existing literature disregards non-independence [5, Chapter 4]. This motivates the development of the remaining and key part of the paper.

4. General polynomial expansions: Method

4.1. **The problem of non-independence.** According to [5, Chapter 4], the first step when dealing with a random system is: *characterize the probability space defined by the random inputs by a set of a finite number of mutually independent random variables.* This finite number of independent random variables is often called the germ [6, Chapter 1]. Independence simplifies computations a lot: for random number generation, for stochastic representations based on Karhunen-Loève or gPC expansions, etc.

When the input parameters have a multivariate Gaussian distribution, they can be mapped into independent and standard Normal distributions, via the Cholesky's decomposition of the covariance matrix. For non-Gaussian and non-independent parameters, the Rosenblatt transformation maps the parameters into independent Uniform variables on $[0, 1]$ [36]. But it may not be easy to carry out in practice [5, Chapter 4]. A construction of an orthogonal basis for non-independent inputs was exposed in [6, Chapter 2]. However, this basis is not polynomial, and as a result its treatment may be quite complex. The recent paper [37] used Gram-Schmidt orthogonalization to numerically compute orthogonal polynomials for the non-independent random inputs (a non-tensor gPC basis), and the expansion coefficients were estimated through a non-intrusive interpolation-based collocation strategy. That Gram-Schmidt procedure heavily relied upon non-tensor quadrature approximations.

In this section, the approach focuses on the intrusive procedure suggested in [19]. When the parameters are non-independent, gPC expansions are changed by polynomial expansions with respect to the canonical polynomial basis. The good thing: no Gram-Schmidt procedure is required. The bad thing: the Gram matrix associated to the canonical polynomial basis is ill-conditioned.

4.2. **Polynomial expansions (extension of gPC).** Let $\lambda_1, \ldots, \lambda_d$ be the input random parameters, not necessarily independent. The canonical polynomial basis is considered:

$$\psi_k(\lambda) = \lambda_1^{k_1} \cdots \lambda_d^{k_d},$$

where $k_1, \ldots, k_d \geq 0$ and $k \in \{1, 2, 3, \ldots\}$ is bijectively associated with the multi-index $(k_1, \ldots, k_d)$. The order for the bijection is defined as follows (analogous to gPC): $k_1 + \ldots + k_d \leq \deg$ if and only if $k \leq (\deg + d)!/(\deg! d!)$. By convention, $(k_1, \ldots, k_d) = (0, \ldots, 0)$ corresponds to $k = 1$.

Infinite (Taylor) expansions $q_i(t; \lambda) = \sum_{k=1}^{\infty} Q_{ik}(t)\psi_k(\lambda)$ and $p_i(t; \lambda) = \sum_{k=1}^{\infty} P_{ik}(t)\psi_k(\lambda)$ may not be appropriate. Indeed, such expansions would entail analyticity with respect to λ in the mean-square sense [38, page 99], which might be too strong and are only optimal around $\lambda = 0$. In fact, they would correspond to perturbation expansions when the variation of λ is low [38–41], which are often (but not always [42]) restricted to a few terms (typically degree two) because of the complex handling. Instead, special truncated expansions are considered:

$$q_i^K(t; \lambda) = \sum_{k=1}^{K} Q_{ik}(t)\psi_k(\lambda), \quad p_i^K(t; \lambda) = \sum_{k=1}^{K} P_{ik}(t)\psi_k(\lambda), \tag{4.1}$$

where $K = (\deg + d)!/(\deg! d!)$. The deterministic coefficients (dependent on K) may be determined as follows. Impose, formally, the equality between (4.1) and $(q_i(t;\lambda), p_i(t;\lambda))$, and afterward apply inner products in $\mathrm{L}^2(\Theta, \mathrm{d}\mathbb{P})$:

$$\langle q_i(t;\lambda)\psi_j(\lambda)\rangle = \sum_{k=1}^{K} Q_{ik}(t)\langle \psi_k(\lambda)\psi_j(\lambda)\rangle, \quad \langle p_i(t;\lambda)\psi_j(\lambda)\rangle = \sum_{k=1}^{K} P_{ik}(t)\langle \psi_k(\lambda)\psi_j(\lambda)\rangle. \quad (4.2)$$

Let Ψ_{jk} be the $K \times K$ symmetric, positive definite matrix whose (j,k) entry is $\langle \psi_j(\lambda)\psi_k(\lambda)\rangle$. This is the Gram matrix. Let α_i and β_i be the vectors whose j-th entry is $\langle q_i(t;\lambda)\psi_j(\lambda)\rangle$ and $\langle p_i(t;\lambda)\psi_j(\lambda)\rangle$, respectively. Then

$$Q_i(t) = \Psi^{-1}\alpha_i, \quad P_i(t) = \Psi^{-1}\beta_i,$$

where $Q_i = (Q_{i1}, \ldots, Q_{iK})^\top$ and $P_i = (P_{i1}, \ldots, P_{iK})^\top$. This is the analogue to the gPC coefficients (3.1), for which Ψ was the identity.

Notice that the truncated expansion (4.1), with (4.2), is the best mean-square approximation among the polynomials in λ of degree less than or equal to deg, because $\langle (q_i(t;\lambda) - q_i^K(t;\lambda))\psi_j(\lambda)\rangle = 0$, $1 \le j \le K$; hence there is mean-square convergence of (4.1) as $K \to \infty$ [5, Chapter 3] (when the moment problem for $\lambda_1, \ldots, \lambda_d$ is uniquely solvable).

As occurred with gPC expansions, the main issue here is the ignorance of α_i and β_i, as they depend upon the unknown positions and momenta. It would be possible to apply quadrature rules, but the governing system would need to be solved for each quadrature node (analogously to [15]). The interest is rather on a procedure that, somehow, imitates the Galerkin projection approach for gPC [19]. This is the aim of the following subsection. The coefficients will verify a deterministic system, which will be divergence free, and volume preserving as a result [23].

4.3. **Truncating the expansions (imitation of the Galerkin projection technique).** Consider (4.1). These are truncated sums at level $K = (\deg + d)!/(\deg! d!)$, where deg is the maximum degree of the polynomial sum. The deterministic coefficients (dependent on K) are obtained by imitating the Galerkin projection technique. That is, it is formally assumed that the sums (4.1) solve the system (2.1), and next, inner products are applied:

$$\sum_{k=1}^{K} \dot{Q}_{ik}(t)\Psi_{jk} = \langle \frac{\partial H}{\partial p_i}(q^K(t;\lambda), p^K(t;\lambda);\lambda)\psi_j(\lambda)\rangle,$$

$$\sum_{k=1}^{K} \dot{P}_{ik}(t)\Psi_{jk} = \langle -\frac{\partial H}{\partial q_i}(q^K(t;\lambda), p^K(t;\lambda);\lambda)\psi_j(\lambda)\rangle, \quad i = 1, \ldots, n, \quad j = 1, \ldots, K,$$

where $q^K = (q_1^K, \ldots, q_n^K)^\top$ and $p^K = (p_1^K, \ldots, p_n^K)^\top$. Note the key role of the Gram matrix Ψ. In matrix form,

$$\dot{Q}_i(t) = \Psi^{-1}\left(\langle \frac{\partial H}{\partial p_i}(q^K(t;\lambda), p^K(t;\lambda);\lambda)\psi_j(\lambda)\rangle\right)_{j=1}^{K}, \quad (4.3)$$

$$\dot{P}_i(t) = \Psi^{-1}\left(\langle -\frac{\partial H}{\partial q_i}(q^K(t;\lambda), p^K(t;\lambda);\lambda)\psi_j(\lambda)\rangle\right)_{j=1}^{K}, \quad (4.4)$$

where $Q_i = (Q_{i1}, \ldots, Q_{iK})^\top$ and $P_i = (P_{i1}, \ldots, P_{iK})^\top$. These equations are analogous to the Galerkin system from Section 3, except for the (annoying!) presence of Ψ^{-1}. (And when

the input parameters are independent, the Galerkin-based polynomial representations (3.2) and (4.1) coincide for every K [21].) The initial positions and momenta of the motion of the coefficients are

$$Q_i(0) = \Psi^{-1}\left(\langle q_i(0;\lambda)\psi_j(\lambda)\rangle\right)_{j=1}^{K}, \quad P_i(0) = \Psi^{-1}\left(\langle p_i(0;\lambda)\psi_j(\lambda)\rangle\right)_{j=1}^{K}.$$

Once the polynomial representations for the coordinates and the momenta are set, the mean and the standard deviation can be approximated as follows:

$$\langle q_i(t;\lambda)\rangle \approx \langle q_i^K(t;\lambda)\rangle = \sum_{k=1}^{K} Q_{ik}(t)\langle\psi_k(\lambda)\rangle, \tag{4.5}$$

$$\sigma[q_i(t;\lambda)] \approx \sigma[q_i^K(t;\lambda)] = \sqrt{\sum_{k_1,k_2=1}^{K} Q_{ik_1}(t)Q_{ik_2}(t)\Psi_{k_1k_2}}. \tag{4.6}$$

(The analogous formulas hold for the momenta.) Other statistics, or the probability density, can be estimated by a simple post-processing; nothing but polynomial evaluations at realizations are involved.

The deterministic system (4.3)–(4.4) derived for the coefficients is examined in the following theorem from a geometric perspective.

Theorem 4.1. *System* (4.3)–(4.4) *is divergence free, therefore it is volume preserving. In general, it is not Hamiltonian. The average of the Hamiltonian H from the original model* (2.1) *is a first integral of* (4.3)–(4.4)*. If H is an even function of momenta, then system* (4.3)–(4.4) *has a reversible flow.*

Proof. System (4.3)–(4.4) is rewritten as

$$\dot{Q}_{il} = \sum_{j=1}^{K}(\Psi^{-1})_{lj}\langle\frac{\partial H}{\partial p_i}(q^K,p^K;\lambda)\psi_j(\lambda)\rangle = F_{il}(Q,P),$$

$$\dot{P}_{il} = -\sum_{j=1}^{K}(\Psi^{-1})_{lj}\langle\frac{\partial H}{\partial q_i}(q^K,p^K;\lambda)\psi_j(\lambda)\rangle = G_{il}(Q,P).$$

The notation F_{il} and G_{il} identifies the vector field (F,G) componentwise. To check that the divergence of (F,G) is zero, just compute

$$\frac{\partial F_{il}}{\partial Q_{il}} + \frac{\partial G_{il}}{\partial P_{il}}$$
$$= \sum_{j=1}^{K}(\Psi^{-1})_{lj}\langle\frac{\partial^2 H}{\partial q_i\partial p_i}(q^K,p^K;\lambda)\psi_l(\lambda)\psi_j(\lambda)\rangle - \sum_{j=1}^{K}(\Psi^{-1})_{lj}\langle\frac{\partial^2 H}{\partial p_i\partial q_i}(q^K,p^K;\lambda)\psi_l(\lambda)\psi_j(\lambda)\rangle = 0,$$

and add over $i\in\{1,\dots,n\}$ and $l\in\{1,\dots,K\}$. The key fact here is the equality of the cross partial derivatives of H (which gives rise to zero divergence for Hamiltonian systems (2.1) as well).

Let us see that system (4.3)–(4.4) is not Hamiltonian in general. Let

$$Q = \begin{pmatrix} Q_1 \\ \vdots \\ Q_n \end{pmatrix} \in \mathbb{R}^{nK}, \quad P = \begin{pmatrix} P_1 \\ \vdots \\ P_n \end{pmatrix} \in \mathbb{R}^{nK}, \quad X = \begin{pmatrix} Q \\ P \end{pmatrix} \in \mathbb{R}^{2nK},$$

$$J = \begin{pmatrix} O_{nK} & I_{nK} \\ -I_{nK} & O_{nK} \end{pmatrix}, \quad \hat{\Psi} = \text{diagonal}(\overbrace{\Psi, \dots, \Psi}^{2n \text{ times}}) \in \mathbb{R}^{2nK \times 2nK}.$$

Consider the function $\tilde{H}$, defined as the average of H [17]:

$$\tilde{H}(Q,P) = \langle H(\left(\sum_{k=1}^{K} Q_{ik}\psi_k(\lambda)\right)_{i=1}^{n}, \left(\sum_{k=1}^{K} P_{ik}\psi_k(\lambda)\right)_{i=1}^{n}; \lambda)\rangle. \tag{4.7}$$

Then the system (4.3)–(4.4) is equivalent, in compact writing, to

$$\dot{X} = \hat{\Psi}^{-1} J \nabla \tilde{H}(X), \tag{4.8}$$

where ∇ is the gradient operator (in column format). Let $\varphi_t(X_0)$, $X_0 = (Q(0), P(0))$, be the flow associated to (4.8). The system is Hamiltonian if and only if φ_t is symplectic (recall definition (2.2)). To ascertain non-symplecticity, note that, from $\dot{\varphi}_t(X_0) = \hat{\Psi}^{-1} J \nabla \tilde{H}(\varphi_t(X_0))$, it holds

$$\dot{\varphi}_t'(X_0) = \hat{\Psi}^{-1} J \tilde{H}''(\varphi_t(X_0))\varphi_t'(X_0),$$

where the prime denotes the Jacobian matrix and the double prime denotes the Hessian matrix. Then

$$\begin{aligned}
&\frac{\mathrm{d}}{\mathrm{d}t}\left(\varphi_t'(X_0)^\top J \varphi_t'(X_0)\right) = \dot{\varphi}_t'(X_0)^\top J \varphi_t'(X_0) + \varphi_t'(X_0)^\top J \dot{\varphi}_t'(X_0) \\
&= \varphi_t'(X_0)^\top \tilde{H}''(\varphi_t(X_0)) \underbrace{J^\top}_{=-J} \hat{\Psi}^{-1} J \varphi_t'(X_0) + \varphi_t'(X_0)^\top J \hat{\Psi}^{-1} J \tilde{H}''(\varphi_t(X_0))\varphi_t'(X_0) \\
&= \varphi_t'(X_0)^\top \tilde{H}''(\varphi_t(X_0)) \hat{\Psi}^{-1} \varphi_t'(X_0) - \varphi_t'(X_0)^\top \hat{\Psi}^{-1} \tilde{H}''(\varphi_t(X_0))\varphi_t'(X_0) \\
&= \varphi_t'(X_0)^\top [\tilde{H}''(\varphi_t(X_0)), \hat{\Psi}^{-1}] \varphi_t'(X_0) \neq 0,
\end{aligned}$$

where $[\cdot,\cdot]$ denotes the commutator. (Notice that, if Ψ were I_K as in the gPC setting, then the commutator would be zero and the flow symplectic, as expected.)

To check that the average $\tilde{H}$ given by (4.7) is a first integral, differentiate its value along the flow:

$$\frac{\mathrm{d}}{\mathrm{d}t}\tilde{H}(X(t)) = (\nabla \tilde{H}(X(t)))^\top \dot{X}(t) = (\nabla \tilde{H}(X(t)))^\top \hat{\Psi}^{-1} J \nabla \tilde{H}(X).$$

Taking into account the block diagonal form of $\hat{\Psi}^{-1}$, the structure of $\hat{\Psi}^{-1}J$ is, by blocks in half,

$$\begin{pmatrix} O_{nK} & \star \\ -\star & O_{nK} \end{pmatrix}.$$

This implies that $z^\top \hat{\Psi}^{-1} J z = 0$ for every column vector $z \in \mathbb{R}^{2nK}$. In particular,

$$\frac{\mathrm{d}}{\mathrm{d}t}\tilde{H}(X(t)) = 0.$$

Finally, if $H(q,p;\lambda) = H(q,-p;\lambda)$, then

$$\frac{\partial H}{\partial p_i}(q,p;\lambda) = -\frac{\partial H}{\partial p_i}(q,-p;\lambda), \quad \frac{\partial H}{\partial q_i}(q,p;\lambda) = \frac{\partial H}{\partial q_i}(q,-p;\lambda).$$

For $\dot{X} = E(X)$, $E = (F^\top, G^\top)^\top$ and $S(Q,P) = (Q,-P)$, the identity $S \circ E = -E \circ S$ holds. By [18, Theorem 2.10], this identity is equivalent to the reversibility of the flow. This completes the proof of the theorem. □

Remark 4.2. In the theorem, an alternative proof for the non-Hamiltonian character of system (4.3)–(4.4) may go in line with classical results on the surjectivity of the gradient operator [23, Lemma 2.7]. A system is Hamiltonian if and only if the Jacobian of its vector field is symmetric. In the previous proof, $F_{il}(Q,P)$ and $G_{il}(Q,P)$ are the components of the vector field. Notice that, for instance,

$$\frac{\partial G_{11}}{\partial Q_{12}}(Q,P) \neq \frac{\partial G_{12}}{\partial Q_{11}}(Q,P)$$

unless $\Psi = I_K$, so the vector field cannot arise from a gradient. The calculations for these partial derivatives are shown here:

$$\begin{aligned}
\frac{\partial G_{11}}{\partial Q_{12}}(Q,P) &= -\sum_{j=1}^{K}(\Psi^{-1})_{1j}\langle\psi_j(\lambda)\frac{\partial}{\partial Q_{12}}\frac{\partial H}{\partial q_1}(q^K(t;\lambda),p^K(t;\lambda);\lambda)\rangle \\
&= -\sum_{j=1}^{K}(\Psi^{-1})_{1j}\langle\psi_j(\lambda)\left(\sum_{r=1}^{n}\frac{\partial^2 H}{\partial q_r\partial q_1}(q^K(t;\lambda),p^K(t;\lambda);\lambda)\frac{\partial q_r^K(t;\lambda)}{\partial Q_{12}}\right)\rangle \\
&= -\sum_{j=1}^{K}(\Psi^{-1})_{1j}\langle\psi_j(\lambda)\frac{\partial^2 H}{\partial q_1\partial q_1}(q^K(t;\lambda),p^K(t;\lambda);\lambda)\psi_2(\lambda)\rangle,
\end{aligned}$$

$$\begin{aligned}
\frac{\partial G_{12}}{\partial Q_{11}}(Q,P) &= -\sum_{j=1}^{K}(\Psi^{-1})_{2j}\langle\psi_j(\lambda)\frac{\partial}{\partial Q_{11}}\frac{\partial H}{\partial q_1}(q^K(t;\lambda),p^K(t;\lambda);\lambda)\rangle \\
&= -\sum_{j=1}^{K}(\Psi^{-1})_{2j}\langle\psi_j(\lambda)\left(\sum_{r=1}^{n}\frac{\partial^2 H}{\partial q_r\partial q_1}(q^K(t;\lambda),p^K(t;\lambda);\lambda)\frac{\partial q_r^K(t;\lambda)}{\partial Q_{11}}\right)\rangle \\
&= -\sum_{j=1}^{K}(\Psi^{-1})_{2j}\langle\psi_j(\lambda)\frac{\partial^2 H}{\partial q_1\partial q_1}(q^K(t;\lambda),p^K(t;\lambda);\lambda)\psi_1(\lambda)\rangle.
\end{aligned}$$

This concludes the remark.

The rigorous mathematical proof of mean-square convergence for the sums (4.1) whose coefficients satisfy the system (4.3)–(4.4) is not an easy issue, and it is not the hope to solve the problem completely. As already commented, the case of gPC expansions and $\Psi = I_K$ was investigated in [34]. Therein a Lipschitz condition of the corresponding vector field was assumed. Now the purpose is to generalize this reference to the canonical polynomial basis. This is done by mapping the canonical polynomial basis into an orthogonal polynomial basis (a non-tensor gPC basis built through Gram-Schmidt orthogonalization). The approach extends [21] to random non-scalar systems, non-independent inputs and non-tensor constructions, and solves challenges encountered in [20].

Theorem 4.3. *Suppose that the sums* (4.1) *with coefficients defined by* (4.2) *converge in root-mean-square at least exponentially fast, namely as* e^{-K}*. (This is known for smooth dependence of the Hamiltonian* H *in* (2.1) *with respect to the parameters* λ*.) Assume also that* H *possesses first partial derivatives that are globally Lipschitz with respect to positions and momenta in root-mean-square. Then the sums* (4.1) *whose coefficients satisfy the system* (4.3)–(4.4) *converge in mean-square.*

Proof. From the canonical basis $\{\psi_k(\lambda)\}_{k=1}^{\infty}$, an orthogonal basis $\{\phi_k(\lambda)\}_{k=1}^{\infty}$ is constructed in $\mathrm{L}^2(\Theta, \mathrm{d}\mathbb{P})$ by Gram-Schmidt orthogonalization:

$$\phi_1(\lambda) = \psi_1(\lambda) = 1,$$

$$\phi_k(\lambda) = \psi_k(\lambda) - \sum_{j=1}^{k-1} \frac{\langle \psi_k(\lambda)\phi_j(\lambda)\rangle}{\langle \phi_j(\lambda)^2\rangle}\phi_j(\lambda), \quad k \geq 2.$$

It may be assumed that $\langle \phi_k(\lambda)^2\rangle = 1$.

Write each element of the basis $\{\psi_k(\lambda)\}_{k=1}^{\infty}$ in terms of $\{\phi_k(\lambda)\}_{k=1}^{\infty}$:

$$\psi_k(\lambda) = \sum_{j\geq 1} R_{kj}\phi_j(\lambda).$$

Notice that $\Psi_{kl} = \langle \psi_k(\lambda)\psi_l(\lambda)\rangle = \sum_{j=1}^{K} R_{kj}R_{lj} = (RR^\top)_{kl}$. That is, $\Psi = RR^\top$, where $R = (R_{kj})_{1\leq k,j\leq K}$. Since R is invertible (because it is a change-of-basis matrix), $\Psi^{-1} = (R^\top)^{-1}R^{-1}$. This identity will be used later.

We have

$$q_i^K(t;\lambda) = \sum_{k=1}^{K} Q_{ik}(t)\psi_k(\lambda) = \sum_{j=1}^{K}\left(\sum_{k=1}^{K} Q_{ik}(t)R_{kj}\right)\phi_j(\lambda).$$

Let

$$\hat{Q}_{ij}(t) = \sum_{k=1}^{K} Q_{ik}(t)R_{kj}$$

be the coefficient of the sum with respect to the orthogonal basis. Analogous formulas hold for $p_i^K(t;\lambda)$ and its coefficients $\hat{P}_{ij}(t)$.

By assuming that $Q_i(t)$ and $P_i(t)$ satisfy system (4.3)–(4.4), let us see which system $\hat{Q}_i(t) = (\hat{Q}_{i1}(t), \ldots, \hat{Q}_{iK})^\top$ and $\hat{P}_i(t) = (\hat{P}_{i1}(t), \ldots, \hat{P}_{iK})^\top$ satisfy. Differentiate:

$$\begin{aligned}
\dot{\hat{Q}}_{ij}(t) &= \sum_{k=1}^{K} \dot{Q}_{ik}(t)R_{kj} = \sum_{k=1}^{K}\left(\sum_{m=1}^{K}(\Psi^{-1})_{km}\langle \frac{\partial H}{\partial p_i}(q^K(t;\lambda), p^K(t;\lambda);\lambda)\psi_m(\lambda)\rangle\right)R_{kj} \\
&= \langle \frac{\partial H}{\partial p_i}(q^K(t;\lambda), p^K(t;\lambda);\lambda)\sum_{m=1}^{K}\left(\sum_{k=1}^{K}(\Psi^{-1})_{km}R_{kj}\right)\psi_m(\lambda)\rangle \\
&= \langle \frac{\partial H}{\partial p_i}(q^K(t;\lambda), p^K(t;\lambda);\lambda)\sum_{m=1}^{K}(R^\top\Psi^{-1})_{jm}\psi_m(\lambda)\rangle \\
&= \langle \frac{\partial H}{\partial p_i}(q^K(t;\lambda), p^K(t;\lambda);\lambda)\sum_{r=1}^{K}(R^\top\Psi^{-1}R)_{jr}\phi_r(\lambda)\rangle \\
&= \langle \frac{\partial H}{\partial p_i}(q^K(t;\lambda), p^K(t;\lambda);\lambda)\sum_{r=1}^{K}(I_K)_{jr}\phi_r(\lambda)\rangle \\
&= \langle \frac{\partial H}{\partial p_i}(q^K(t;\lambda), p^K(t;\lambda);\lambda)\phi_j(\lambda)\rangle.
\end{aligned}$$

This is the Galerkin system for gPC bases. Therefore, polynomial representations in terms of the canonical polynomial basis coincide with those in terms of orthogonal polynomials. This extends [21] to any situation.

Thus, the convergence of the sums (4.1) with coefficients defined by (4.3)–(4.4) can be studied by assuming, without loss of generality, that the basis is orthogonal and the Gram matrix is the identity. This is a key advance. The arguments of [34] can then be applied. Let us do so.

Only within this proof, let us denote by the superscript K the coefficients and expansions corresponding to (4.3)–(4.4) in this Subsection 4.3 (Q_i^K, P_i^K, q_i^K, p_i^K), and by the superscripts ∞, K the coefficients and expansions corresponding to (4.2) in Subsection 4.2 ($Q_i^{\infty,K}$, $P_i^{\infty,K}$, $q_i^{\infty,K}$, $p_i^{\infty,K}$). These distinctions are made to mix coefficients and expansions in inequalities. The superscript ∞ simply reflects that, within the context of Subsection 4.2, there is convergence as K grows. Without loss of generality, let us assume here in this part of the proof that Ψ is the identity matrix and the basis is orthonormal. Denote the root-mean-square norm in $\mathrm{L}^2(\Theta, \mathrm{d}\mathbb{P})$ by $\|\cdot\|_{\text{m.s.}}$. Denote the Euclidean norm of vectors by $\|\cdot\|_e$. We have:

$$
\begin{aligned}
&\|q_i(t;\lambda) - q_i^K(t;\lambda)\|_{\text{m.s.}} - \|q_i(t;\lambda) - q_i^{\infty,K}(t;\lambda)\|_{\text{m.s.}} \leq \|q_i^{\infty,K}(t;\lambda) - q_i^K(t;\lambda)\|_{\text{m.s.}} \\
&= \left\| \sum_{k=1}^{K} \left(Q_{ik}^{\infty,K}(t) - Q_{ik}^K(t) \right) \psi_k(\lambda) \right\|_{\text{m.s.}} = \|Q_i^{\infty,K}(t) - Q_i^K(t)\|_e \\
&= \left\| \left(\langle \psi_j(\lambda) \int_0^t \left(\frac{\partial H}{\partial p_i}(q(\tau;\lambda), p(\tau;\lambda);\lambda) - \frac{\partial H}{\partial p_i}(q^K(\tau;\lambda), p^K(\tau;\lambda);\lambda) \right) \mathrm{d}\tau \rangle \right)_{j=1}^{K} \right\|_e \\
&\leq \left\| \int_0^t \left(\frac{\partial H}{\partial p_i}(q(\tau;\lambda), p(\tau;\lambda);\lambda) - \frac{\partial H}{\partial p_i}(q^K(\tau;\lambda), p^K(\tau;\lambda);\lambda) \right) \mathrm{d}\tau \right\|_{\text{m.s.}} \sqrt{K} \\
&\leq L\sqrt{K} \int_0^t \left(\max_{1\leq m\leq n} \|q_m(\tau;\lambda) - q_m^K(\tau;\lambda)\|_{\text{m.s.}} + \max_{1\leq m\leq n} \|p_m(\tau;\lambda) - p_m^K(\tau;\lambda)\|_{\text{m.s.}} \right) \mathrm{d}\tau,
\end{aligned}
$$

where L is the Lipschitz constant. Analogous inequalities apply for the momenta. For convenience of notation, let

$$
\Xi^K(t) = \max_{1\leq m\leq n} \|q_m(\tau;\lambda) - q_m^K(\tau;\lambda)\|_{\text{m.s.}} + \max_{1\leq m\leq n} \|p_m(\tau;\lambda) - p_m^K(\tau;\lambda)\|_{\text{m.s.}}
$$

and

$$
\Xi^{\infty,K}(t) = \max_{1\leq m\leq n} \|q_m(\tau;\lambda) - q_m^{\infty,K}(\tau;\lambda)\|_{\text{m.s.}} + \max_{1\leq m\leq n} \|p_m(\tau;\lambda) - p_m^{\infty,K}(\tau;\lambda)\|_{\text{m.s.}}.
$$

Then, in short,

$$
\Xi^K(t) \leq \Xi^{\infty,K}(t) + 2L\sqrt{K} \int_0^t \Xi^K(\tau)\, \mathrm{d}\tau.
$$

By Gronwall's inequality,

$$
\Xi^K(t) \leq \Xi^{\infty,K}(t) + 2L\sqrt{K} \int_0^t \Xi^{\infty,K}(\tau) \mathrm{e}^{2L\sqrt{K}\,(t-\tau)} \mathrm{d}\tau.
$$

By hypothesis, $\Xi^{\infty,K}$ converges to zero at least exponentially fast. Consequently, Ξ^K converges to zero. This is exactly the goal of the theorem. □

Remark 4.4. The Lognormal distribution is not determined by its moments. It is known that gPC expansions with respect to the Lognormal density, which are constructed in terms of Stieltjes-Wigert polynomials, do not converge in mean-square [12]. Consider the harmonic oscillator $\ddot{q} + q = 0$, with mass and angular frequency equal to 1, $q(0) = 1/\lambda$, and $\dot{q}(0) = 0$. The solution is $q(t) = q(0)\cos t$. At $t = 1$, the solution is $q(1) = 1/\lambda$. Let $\lambda \sim \mathrm{e}^{\mathrm{Normal}(0,1)}$ and $\{\phi_k(\lambda)\}_{k=1}^{\infty}$ its orthonormal gPC basis. In [12, Proposition 4.2], it was proved that

$$\left\| q(1) - \sum_{k=1}^{K} \langle q(1)\phi_k(\lambda)\rangle \phi_k(\lambda) \right\|_{\mathrm{m.s.}} \geq \sqrt{\mathrm{e}^2 - \frac{\mathrm{e}^2}{\mathrm{e}-1}} > 0.$$

The truncated gPC sum $\sum_{k=1}^{K} \langle q(1)\phi_k(\lambda)\rangle \phi_k(\lambda)$ is the best mean-square approximation to $q(1)$ among the polynomials in λ of degree less than or equal to $\deg = K - 1$. Hence

$$\left\| q(1) - \sum_{k=1}^{K} Q_{1k}(1)\psi_k(\lambda) \right\|_{\mathrm{m.s.}} \geq \left\| q(1) - \sum_{k=1}^{K} \langle q(1)\phi_k(\lambda)\rangle \phi_k(\lambda) \right\|_{\mathrm{m.s.}} \geq \sqrt{\mathrm{e}^2 - \frac{\mathrm{e}^2}{\mathrm{e}-1}} > 0.$$

The lesson is to be careful with the input probability distributions and ensure that the polynomial representations obtained for the output give accurate estimates of the statistics.

Remark 4.5. There are examples for which the position is not mean-square integrable (its variance is infinite) if the root-mean-square Lipschitz condition for the first partial derivatives of the Hamiltonian does not hold. Thus, in some sense, the conditions imposed in Theorem 4.3 are quite sharp. Consider $\ddot{q} = \zeta q$, $q(0) = q_0$, $\dot{q}(0) = 0$, where $\lambda = (\zeta, q_0)$ is the random vector of input parameters. It is assumed that ζ is positive and unbounded and q_0 is mean-square integrable. The solution is $q(t) = q_0 \cosh(\sqrt{\zeta}\, t)$. The Hamiltonian is $H(q,p) = p^2/2 - \zeta q^2/2$. The partial derivative $\partial H/\partial q = -\zeta q$ is not root-mean-square Lipschitz, because ζ is unbounded. On the other hand, given any $t > 0$, it is not possible to have $q(t) \in \mathrm{L}^2(\Theta, \mathrm{d}\mathbb{P})$ for every $q_0 \in \mathrm{L}^2(\Theta, \mathrm{d}\mathbb{P})$; otherwise $\cosh(\sqrt{\zeta}\, t)$, and therefore ζ, would necessarily be bounded. This is a consequence of the closed graph theorem from functional analysis [1]. An explicit example is the following. Set $q_0 = 1$, $t = 1$, and $\sqrt{\zeta}$ with Exponential distribution of mean value 1 (density e^{-z} on $[0, \infty)$). Then $\langle q(1)\rangle = \langle \cosh(\sqrt{\zeta})\rangle = \int_0^{\infty} \cosh(z)\mathrm{e}^{-z}\, \mathrm{d}z = \infty$; that is, the mean (and the variance) is infinite.

4.4. **Numerical aspects: Possibilities and problems.** The numerical aspects of gPC expansions and Galerkin projections have been deeply studied in the literature. The Galerkin system for the coefficients, which is larger than the original system, may be difficult to solve in practice. It may require searching for new algorithms and implementing new codes for an efficient resolution. When these are available, then the Galerkin approach is somehow optimal [5]. This is the case of random Hamiltonian systems, whose associated Galerkin system is also Hamiltonian and symplectic integrators can be applied [17]. The Galerkin projections converge at spectral rate, being exponential for smooth dynamics, though the approximations become severely affected by the magnitude of the time variable and the degree of randomness. A single resolution of the Galerkin system affords a polynomial representation

[1] Let $\xi = \cosh(\sqrt{\zeta}\, t)$. If $q(t) \in \mathrm{L}^2(\Theta, \mathrm{d}\mathbb{P})$ for every $q_0 \in \mathrm{L}^2(\Theta, \mathrm{d}\mathbb{P})$, then the map $\mathrm{L}^2(\Theta, \mathrm{d}\mathbb{P}) \to \mathrm{L}^2(\Theta, \mathrm{d}\mathbb{P})$, $q_0 \mapsto q_0\xi$, is well-defined and linear. Its graph is closed. Then it is continuous: $\|q_0\xi\|_{\mathrm{m.s.}} \leq C\|q_0\|_{\mathrm{m.s.}}$, for certain constant $C > 0$. This inequality holds for any q_0, even if its norm is not finite. For $q_0 = \xi^m$, $m \geq 0$ integer, the inequalities $\|\xi^{m+1}\|_{\mathrm{m.s.}} \leq C\|\xi^m\|_{\mathrm{m.s.}}$ are obtained. These recursive inequalities yield $(\|\xi^m\|_{\mathrm{m.s.}})^{1/m} \leq C$. By letting $m \to \infty$, this implies that $|\xi| \leq C$ almost surely.

of the solution, so a huge improvement over Monte Carlo and quadrature methods may be achieved. From the Galerkin projection, the mean and the variance are the statistics more straightforward. Other than that, Monte Carlo simulation can be conducted on the Galerkin projection, which is a simple exercise in polynomial evaluation, to derive other statistics and the probability density.

As an attempt to generalize gPC expansions and Galerkin projections for non-independent inputs, expansions in terms of the canonical polynomial basis have been proposed. Sums (4.1) with coefficients defined by (4.2) conform the best mean-square approximations in the polynomial field, and mean-square convergence is expected by following the reasoning of [5, Chapter 3]. When, in lieu of employing (4.2), an imitation of the Galerkin approach is pursued, the associated system for the coefficients (4.3)–(4.4) is volume preserving but non-Hamiltonian. Thereby, volume-preserving integrators are applicable. Numerically, there will be evidence that the method works for uncertainty quantification, showing similar features to gPC-based methods. As a simple post-processing of the polynomial representation, the statistical content of the solution can be estimated: the mean and the variance through closed-form formulas, and other statistics and the probability density through Monte Carlo simulation.

The deterministic system of the expansion coefficients (4.3)–(4.4) is a set of $2nK$ coupled differential equations. If an efficient solver is used, the cost is slightly more than $2nK$ single deterministic integrations of the governing model (2.1). On the other hand, if Monte Carlo simulation is applied on (2.1) with M realizations, then $2nM$ deterministic integrations are taken. When $K < M$, then Monte Carlo simulation is more costly. In addition, the slow convergence rate of Monte Carlo simulation should be taken into account. For example, suppose only one input random parameter. Then $K = \deg + 1$, where deg is the maximum degree of the polynomial basis. Such deg is normally ≤ 5 for a relative error of 10^{-3} for the mean and the standard deviation. For such accuracy, Monte Carlo simulation necessitates around $M = \mathscr{O}(10^5) \sim \mathscr{O}(10^6)$ integrations. Thus, the advantage of polynomial representations is obvious. If there are two input random parameters, then $K = (\deg + 1)(\deg + 2)/2$. If $\deg = 5$, then $K = 21$, and the gain of polynomial representations is still evident. Nonetheless, when the number of input random parameters is not low, the efficiency of the polynomial representations may be degraded. Additionally, recall that this efficiency is constrained to moderately large independent variable and to smooth dynamics, whereas Monte Carlo simulation is insensitive to these conditions.

A major difference of the expansions discussed here compared to gPC and Galerkin projections is the avoidance of a (challenging) Gram-Schmidt orthogonalization procedure but the presence of the Gram matrix associated to the canonical polynomial basis. The Gram matrix may be highly ill-conditioned [22]. For example, if an input parameter has a Uniform distribution on the range $[0, 1]$, then the Gram matrix is the well-known Hilbert matrix, whose condition number grows exponentially [43–47]. This may produce instabilities in numerical computations [21]. Nevertheless, polynomial expansions are expected to converge exponentially, as occurs with Galerkin projections, so sum representations with few basis terms should be enough. That is, the Gram matrix may be of moderate size and no problems should then arise.

An important issue to be mentioned, which is not constrained to expansions with respect to the canonical polynomial basis, but also affects gPC expansions, is the explicit writing of the system for the coefficients: (3.3)–(3.4) and (4.3)–(4.4). Specifically, the inner products between the vector field of (2.1) and the basis need to be calculated. In general, when the

Hamiltonian H is of polynomial form, the inner products can be computed symbolically, in closed form. For other nonlinear forms, the inner products may require quadratures or Taylor expansions for approximations. These ideas have been developed in [5, Chapter 6], [6, Chapter 4]. However, if sampling is required in a pre-processing stage, maybe a fully non-intrusive method would be better suited. That would depend on the difficulty of the nonlinearity.

The system associated with the coefficients has to be integrated. For orthogonal expansions, the Galerkin system (3.3)–(3.4) is Hamiltonian. Therefore, integration is based on symplectic schemes. For expansions in terms of the canonical polynomial basis, the system (4.3)–(4.4) is volume preserving, but non-Hamiltonian. Part of [23, Chapter 6] is devoted to volume-preserving integrators. Its approach is largely based on [48], which decomposes every divergence-free vector field into Hamiltonian vector fields, so a volume-preserving algorithm is obtained by applying a splitting method with symplectic substeps. Separable problems (4.3)–(4.4), i.e. those of the form $\dot{Q} = F(P)$, $\dot{P} = G(Q)$, which arise from a separable Hamiltonian $H(q,p) = T(p) + V(q)$, are easier to deal with, since the semi-implicit Euler, Störmer-Verlet and some Runge-Kutta methods are volume preserving [23, page 231]. This is not difficult to prove in the present particular case. In fact, it seems that, here, separability is not actually needed by the special structure of (4.3)–(4.4). Since the composition of volume-preserving methods is volume preserving, the focus is put on the semi-implicit Euler. Consider the version

$$P^{m+1} = P^m - (\Delta t) A \tilde{H}_Q(Q^m, P^{m+1}), \quad Q^{m+1} = Q^m + (\Delta t) A \tilde{H}_P(Q^m, P^{m+1}), \tag{4.9}$$

where Δt is the (constant) step-size, $A = \text{diagonal}(\overbrace{\Psi^{-1}, \ldots, \Psi^{-1}}^{n \text{ times}})$, $\tilde{H}$ is defined as (4.7) (the average of H), $\tilde{H}_Q = \nabla_Q \tilde{H}$, $\tilde{H}_P = \nabla_P \tilde{H}$, and $m \geq 0$ is the iteration step. Then, as in [23, Theorem 3.3],

$$\begin{pmatrix} I_{nK} + (\Delta t) A \tilde{H}_{qp}^\top & O_{nK} \\ -(\Delta t) A \tilde{H}_{pp} & I_{nK} \end{pmatrix} \frac{\partial (P^{m+1}, Q^{m+1})}{\partial (P^m, Q^m)} = \begin{pmatrix} I_{nK} & -(\Delta t) A \tilde{H}_{qq} \\ O_{nK} & I_{nK} + (\Delta t) A \tilde{H}_{qp} \end{pmatrix},$$

where the matrices of second-order partial derivatives are evaluated at (Q^m, P^{m+1}). This implies that

$$\det \left(\frac{\partial (P^{m+1}, Q^{m+1})}{\partial (P^m, Q^m)} \right) = 1,$$

as wanted. The reader should be convinced that system (4.3)–(4.4), despite not being Hamiltonian, possesses a special structure that makes traditional symplectic integrators of use to preserve volume. Not all divergence-free systems satisfy this notable property.

After the obtainment of the final polynomial representation, there are two sources of error: the finite degree of the polynomial basis (i.e. the expansion is finite), and the integrator time-step. For a fixed time-step, there is a polynomial degree for which the global error does not reduce anymore. In general, there should a balance in order not to have a certain error dominant.

Once the system for the coefficients has been integrated and the polynomial representation is obtained, the post-processing stage commences. The statistics are readily obtained, either by closed-form formulas or by Monte Carlo simulation. Expressions (4.5) and (4.6) for the mean and the standard deviation do not pose much difficulty, though these are not as simple as those for orthogonal expansions, (3.5) and (3.6).

5. General polynomial expansions: Examples

In this section, prototypical models from Hamiltonian dynamics are treated: harmonic oscillator, undamped and unforced Duffing oscillator, and simple gravity pendulum. To study the performance of numerical methods designed for forward uncertainty quantification, some input parameters are assumed to have (joint) probability distributions, and afterward the statistical content of the response is obtained. The focus is put on the mean and the standard deviation, due to mean-square convergence. The probability density is also estimated by sampling the polynomial representation. The performance of the polynomial expansions is compared with the standard Monte Carlo method, for moderate time variable.

To solve the (non-Hamiltonian but volume-preserving) system of the expansion coefficients, (4.3)–(4.4), the Störmer-Verlet integrator (which is volume preserving for it) is employed. In the notation of the preceding subsection, the iterations read as follows:

$$\begin{aligned} P^{m+1/2} &= P^m - \frac{\Delta t}{2} A \nabla_Q \tilde{V}(Q^m), \\ Q^{m+1} &= Q^m + (\Delta t) A \tilde{M}^{-1} P^{m+1/2}, \\ P^{m+1} &= P^{m+1/2} - \frac{\Delta t}{2} A \nabla_Q \tilde{V}(Q^{m+1}), \end{aligned}$$

where $\tilde{M}$ and $\tilde{V}$ are the mass matrix and the potential energy of $\tilde{H}$, respectively. This Störmer-Verlet integrator is the composition of semi-implicit Euler and its adjoint with step-size $(\Delta t)/2$ (check from the definition (4.9)). Therefore, it is symmetric, i.e. equal to its adjoint. This mimics the property of exact flows of autonomous systems: $\varphi_{-t}^{-1} = \varphi_t$. This feature is not shared by the corresponding map of many numerical methods.

The Störmer-Verlet integrator used here may be seen as the palindromic composition of flows (splitting algorithm). Consider the systems

$$\dot{Q} = A\tilde{M}^{-1}P, \quad \dot{P} = 0 \quad \Longrightarrow \quad \varphi_t^1(Q(0), P(0)) = (Q(0) + tA\tilde{M}^{-1}P(0), P(0)),$$

$$\dot{Q}(0) = 0, \quad \dot{P} = -A\nabla_Q \tilde{V}(Q) \quad \Longrightarrow \quad \varphi_t^2(Q(0), P(0)) = (Q(0), P(0) - tA\nabla_Q \tilde{V}(Q(0))).$$

Then $\varphi_t^1 \circ S \circ \varphi_t^1 = S$ and $\varphi_t^2 \circ S \circ \varphi_t^2 = S$, that is, the flows are reversible. The Störmer-Verlet algorithm updates values as

$$(Q^{m+1}, P^{m+1}) = (\varphi_{\frac{\Delta t}{2}}^2 \circ \varphi_{\Delta t}^1 \circ \varphi_{\frac{\Delta t}{2}}^2)(Q^m, P^m).$$

Since φ_t^1 and φ_t^2 are volume preserving and reversible, so is the Störmer-Verlet integrator. (Volume preservation was already known.) All these favorable properties, besides the simple formulation, show the strength of the Störmer-Verlet method for numerical integration.

In classical numerical analysis, integrators are usually assessed on the model scalar linear equation $\mathrm{d}y/\mathrm{d}t = ay$. Then, it is hoped that the conclusions apply to nonlinear situations. In fact, if the integrator does not work for the model equation, then it is not useful for more complex problems, for sure. In our setting, the model problem is the harmonic oscillator. It is a linear problem. (Notwithstanding, randomness enters into the equation in a multiplicative manner, so the equation may be seen as nonlinear from the perspective of the random space.) The undamped and unforced Duffing oscillator includes polynomial nonlinearities. The simple gravity pendulum has non-polynomial terms, which forces a special treatment for the inner products in the construction of the coefficients system.

Example 5.1. Let

$$\ddot{q} + \omega^2 q = 0, \quad q(0) = q_0, \quad \dot{q}(0) = 0, \tag{5.1}$$

be a model for the harmonic oscillator, where ω is the angular frequency. Its Hamiltonian is $H(q,p) = \frac{1}{2}(\omega^2 q^2 + p^2)$. It is assumed that $\lambda = (\omega, q_0)$ is a random vector, whose distribution is Dirichlet of parameters $(1, 2, 0.8)$. Its probability density is

$$f_{(\omega,q_0)}(\omega, q_0) = \frac{q_0 \Gamma(19/5)}{(1-\omega-q_0)^{1/5}\Gamma(4/5)}, \quad \omega, q_0 > 0, \quad 1-\omega-q_0 > 0.$$

These inputs are non-independent. Hence the method investigated in this paper is applied. The exact solution $q(t) = q_0 \cos(\omega t)$ serves as validation and testing.

Unlike the deterministic situation, each realization of (ω, q_0) gives rise to a solution $q(t)$ (a sample-path). Some trajectories in phase space are collected in Figure 1, for times $t \in [0, 10]$. These trajectories exhibit significant variability. The aim of uncertainty quantification is to "summarize" this variability from statistical measures.

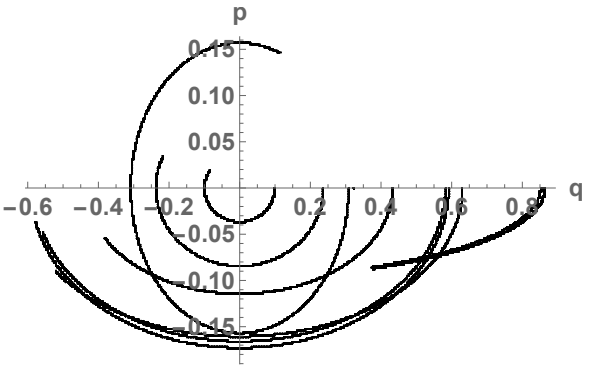

FIGURE 1. Some trajectories of the harmonic oscillator in phase space, for times $t \in [0, 10]$. The realizations of (ω, q_0) have been generated randomly. This figure corresponds to Example 5.1.

In Figure 2, the expectation (the average of Figure 1) and the standard deviation (the dispersion of Figure 1) of the positions and momenta are shown, until time $t = 10$. The figure has been built with polynomial degree 5 and the Störmer-Verlet integrator with step-size $\Delta t = 0.001$. (In a moment it will be checked that these polynomial representations afford faithful estimates of the statistics, by means of error diagrams.)

Figures 3 and 4 report the relative errors in the approximation of the mean and the standard deviation of $q(t)$, for increasing polynomial degrees, up to time $t = 10$, with two different step-sizes, $\Delta t = 0.001$ and $\Delta t = 0.0001$, respectively. A logarithmic scale is used. First, it is observed that, as the time variable t increases, the method looses accuracy. This is an expected fact from other polynomial-based methods. Second, it is appreciated that, for lower Δt, the errors from the pictures decrease slightly. This is because the integration error was higher than the polynomial degree error near $t = 0$ in Figure 3.

Next is highlighted the importance of the integrator in Figure 5. For polynomial degree 1, there are $K = 3$ terms in the expansion, and the system for the coefficients has size 6, with components Q_{1k} and P_{1k}, $k = 1, 2, 3$. This system is solved with different methods: explicit Euler and Heun, which are volume non-preserving, and semi-implicit Euler and Störmer-Verlet. Relative errors on the positions Q_{1k} (max on $k \in \{1, 2, 3\}$) are computed from a

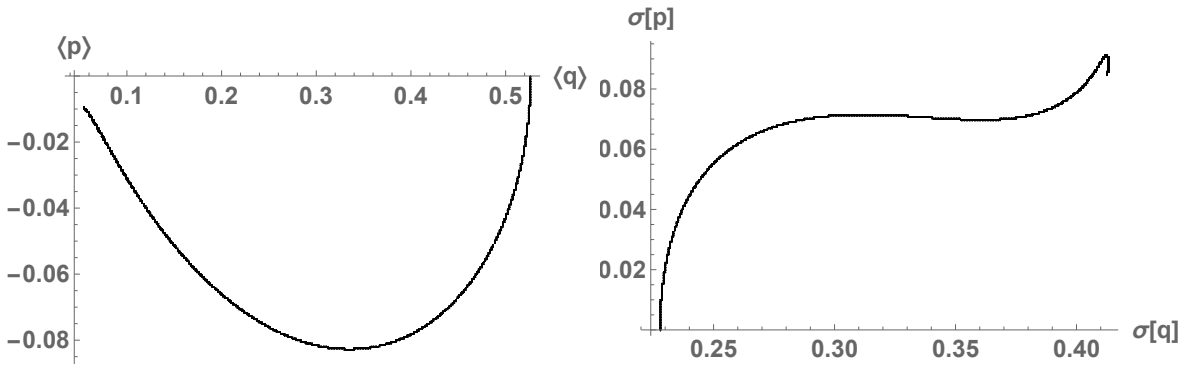

FIGURE 2. Expectation and standard deviation of the positions and momenta, until time $t = 10$. The deterministic system of the expansion coefficients is solved by the Störmer-Verlet integrator, with step-size $\Delta t = 0.001$. This figure corresponds to Example 5.1.

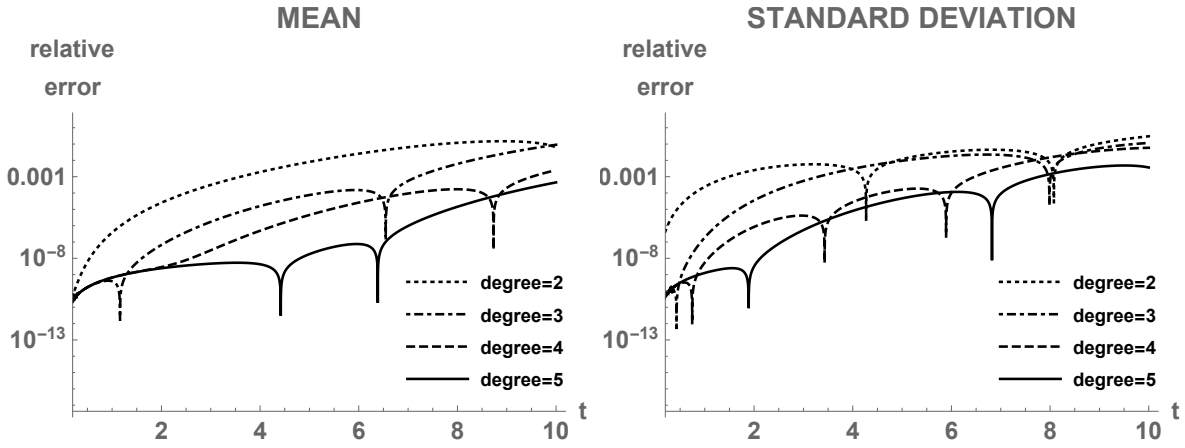

FIGURE 3. Relative errors in the approximation of the mean and the standard deviation of $q(t)$, for increasing polynomial degrees, up to time $t = 10$. The deterministic system of the expansion coefficients is solved by the Störmer-Verlet integrator, with step-size $\Delta t = 0.001$. Logarithmic scale is used. This figure corresponds to Example 5.1.

software built-in function for differential equations with high accuracy. Here Heun's method is defined as follows: for $\dot{X} = E(X)$, where $X = (Q^\top, P^\top)^\top$ and $E = (F^\top, G^\top)^\top$,

$$X^{m+1} = X^m + \frac{\Delta t}{4}\left(E(X^m) + 3E(X^m + (2(\Delta t)/3)E(X^m))\right).$$

The comparison brings out the usefulness of preserving geometric characteristics. Indeed, observe that the errors produced with classical non-geometric integrators are higher (for each order of convergence). In Figure 6, the relative errors

$$\frac{|\tilde{H}(X(t)) - \tilde{H}(X(0))|}{|\tilde{H}(X(0))|} \tag{5.2}$$

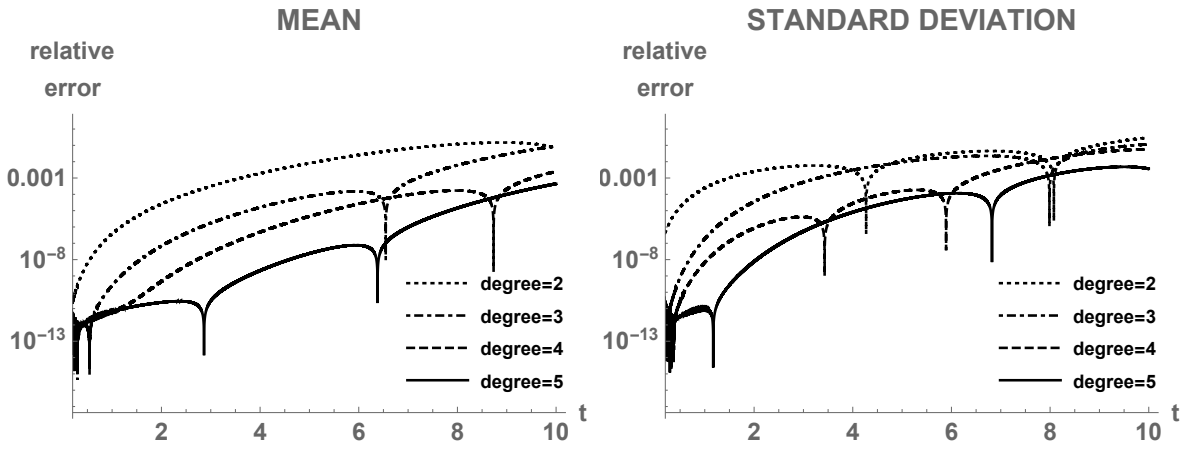

FIGURE 4. Relative errors in the approximation of the mean and the standard deviation of $q(t)$, for increasing polynomial degrees, up to time $t = 10$. The deterministic system of the expansion coefficients is solved by the Störmer-Verlet integrator, with step-size $\Delta t = 0.0001$. Logarithmic scale is used. This figure corresponds to Example 5.1.

are reported, which should ideally be zero (because $\tilde{H}$ in (4.7) is a first integral). Here $\tilde{H}(X(0)) = 625/74936$. Observe that geometric integrators present an oscillating, bounded and lower error. There is an error growth with time in non-geometric integrators.

In Figure 7, relative errors in the sampling of Monte Carlo simulation are shown. For samples of length $10,000$ (upper panels) and $50,000$ (lower panels), the mean error and 95% confidence intervals are depicted. For moderate t, the Monte Carlo simulation cannot attain the convergence order of the polynomial expansions. On the other hand, Figure 8 demonstrates that the accuracy of finite-term Taylor series with respect to λ is not as good as that reported in Figures 3 and 4. Indeed, Taylor series are only optimal around $\lambda = 0$, whereas the technique treated in this paper searches for the best mean-square approximation among the polynomials in λ.

In Figure 9, probability densities are estimated. Kernel density estimation is applied both to the polynomial representation of degree 5 (post-processing) and to $q(t)$ directly. Two times t are selected for exemplification. At time $t = 1$, both densities are indistinguishable at the scale of the figure. But at time $t = 10$, the density of the polynomial representation deviates. This breakdown of the polynomial approximation is analogous to gPC expansions. Furthermore, notice that the rate of convergence of the densities is lower than the mean-square convergence rate from the previous figures.

This example is concluded by illustrating that the rate of mean-square convergence is not equivalent to the rate of almost sure convergence. For realizations $\omega = 1$ and $q_0 = 1$, polynomial approximations of $q(t) = \cos t$ are depicted in Figure 10. The rate of pointwise convergence is slower than the mean-square convergence rate analyzed in the earlier figures. According to [16, Section 6.3], the convergence of gPC expansions for oscillating functions cannot be retained for long; this is a result of the classical approximation theory. The larger t is, the more basis functions one needs to employ in order to keep a given accuracy.

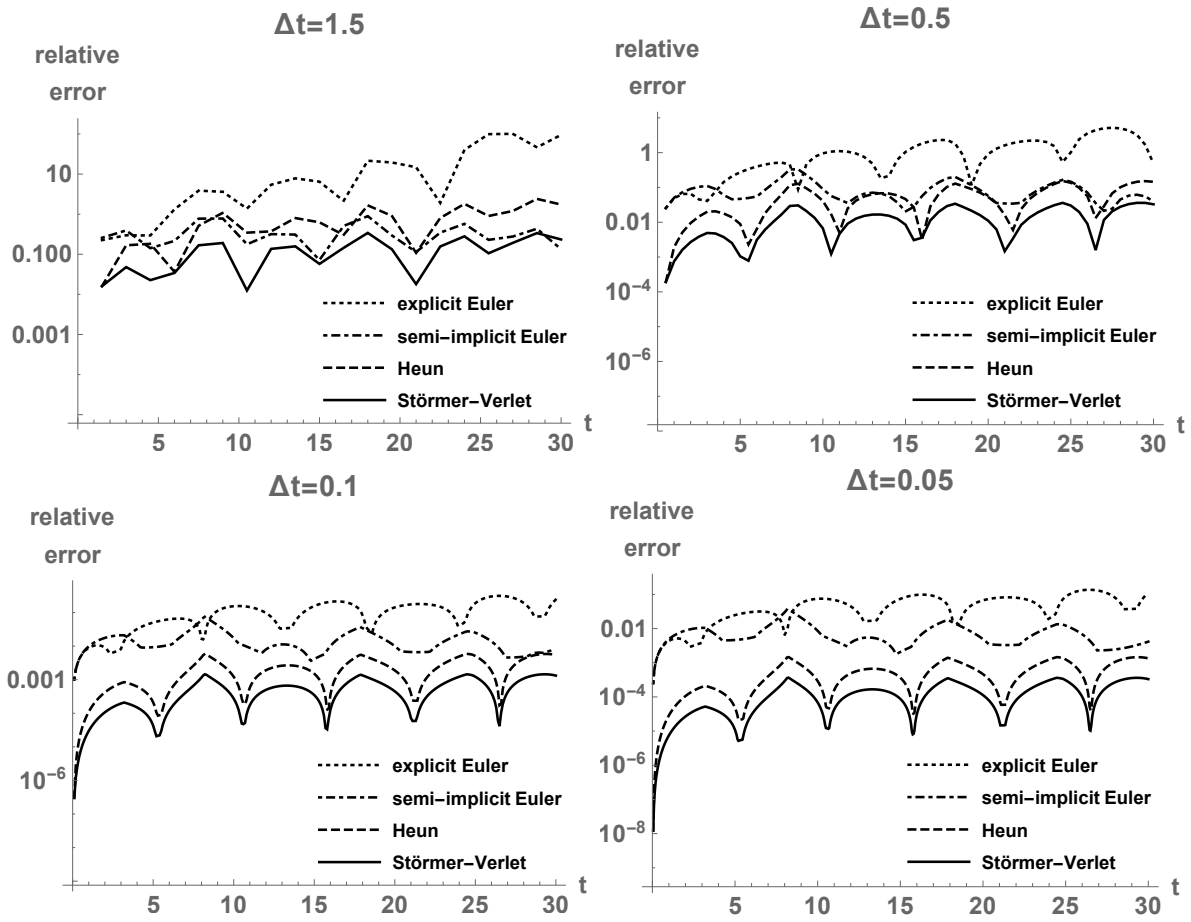

FIGURE 5. Relative errors in the resolution of the system for the coefficients up to time $t = 30$ (coordinates space). The polynomial degree 1 is fixed, so that the system has size 6. Different step-sizes Δt are set, as indicated. Logarithmic scale is used. This figure corresponds to Example 5.1.

Example 5.2. Consider the harmonic oscillator (5.1) again. Now ω and q_0 are independent random variables, with Uniform distribution on $[0, 1]$. The methodology proposed in this paper is applicable. Due to independence, tensor Legendre-type gPC expansions can also be employed. For each degree, both polynomial representations coincide. This is illustrated in Figure 11, with Störmer-Verlet integration of step-size $\Delta t = 0.001$. Thus, polynomial expansions with respect to the canonical basis generalize gPC. Nonetheless, the Gram matrix Ψ associated to the canonical basis is ill-conditioned, and this may ruin computations for large degree. The condition number of Ψ, defined as the ratio between the maximum and minimum eigenvalue, is plotted with the polynomial degree in Figure 12.

Example 5.3. In this example, polynomial nonlinearities are treated via the undamped and unforced Duffing oscillator:

$$\ddot{q} + \alpha q + q^3 = 0, \quad q(0) = q_0, \quad \dot{q}(0) = 0.$$

The potential is more complex than in simple harmonic motion. The parameter α controls the linear stiffness. The cube is the nonlinearity in the restoring force. The Hamiltonian is

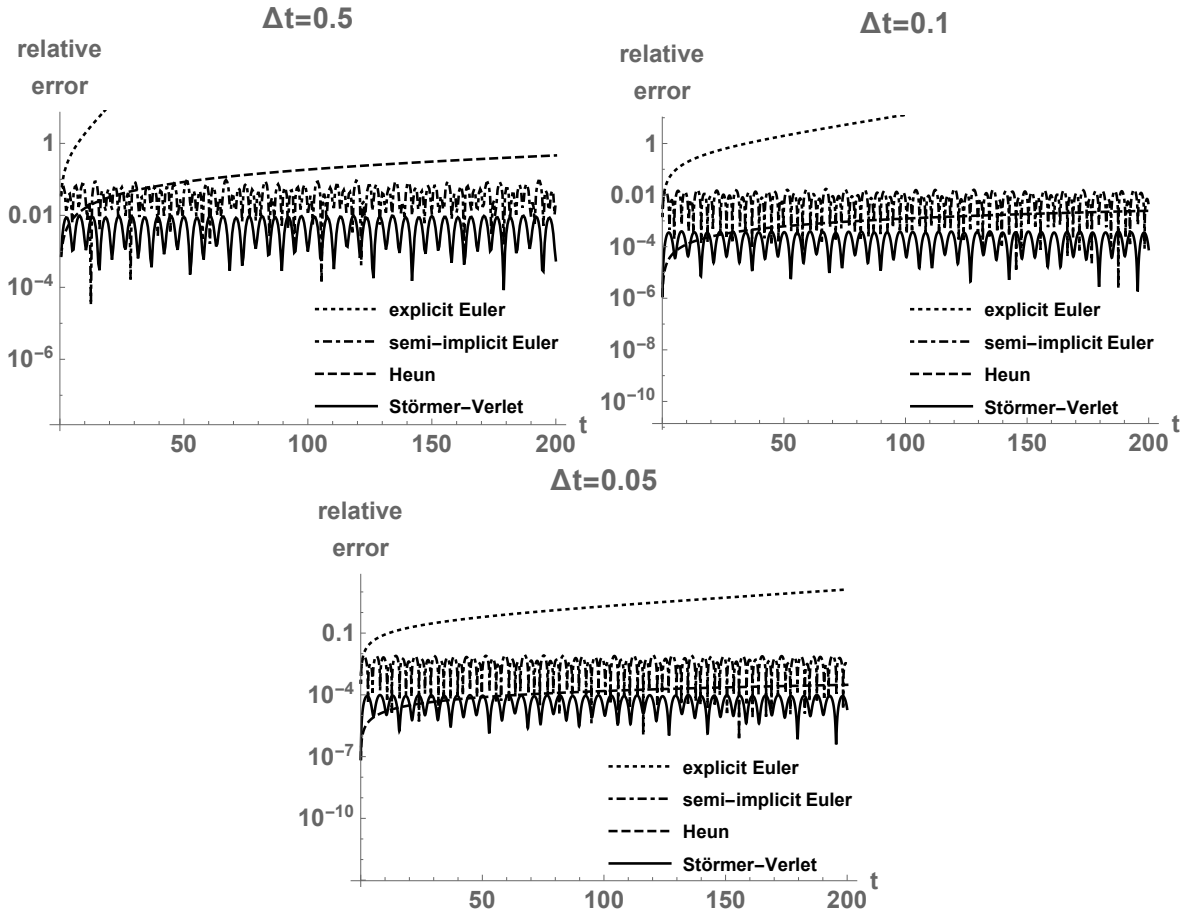

FIGURE 6. Relative errors in $\tilde{H}(X(t))$, where $\tilde{H}$ is the average of H and a first integral, and X is the flow of the system for the coefficients. Times $t \in [0, 200]$ are considered. The polynomial degree 1 is fixed, so that the system has size 6. Different step-sizes Δt are set, as indicated. Logarithmic scale is used. This figure corresponds to Example 5.1.

given by $H(q, p) = p^2/2 + \alpha q^2/2 + q^4/4$. It is assumed that $\lambda = (\alpha, q_0)$ is a random vector, with the same distribution as the first example: Dirichlet of parameters $(1, 2, 0.8)$.

In Figure 13, the evolution of several trajectories in phase space is shown, for different realizations of (α, q_0). Times along $[0, 10]$ are considered.

In Figure 14, the expectation (the average of Figure 13) and the standard deviation (the dispersion of Figure 13) of the positions and momenta are shown, until time 10. Different degrees are reported. For moderate t, the approximations match at the scale of the figure. As the time t advances, more basis terms are required to maintain accuracy.

The reliability of the results is verified by comparing with Monte Carlo simulation. Figure 15 graphs the approximated density functions at $t = 1$. Kernel density estimation has been employed, both to the polynomial representation of degree 4 and to the numeric solution $q(t)$ directly. The densities coincide visually. But as t increased, the accuracy in the density estimation would diminish.

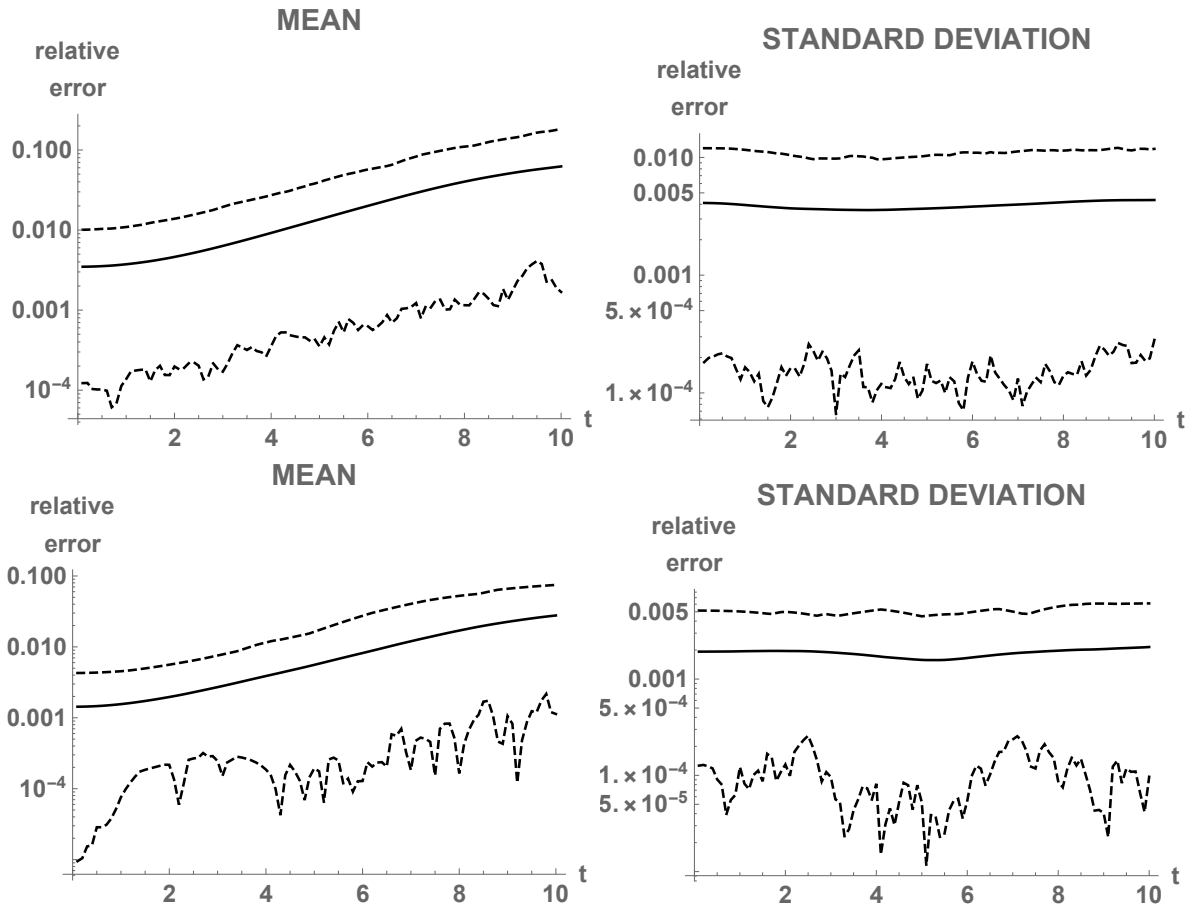

FIGURE 7. Relative errors in the approximation of the mean and the standard deviation of $q(t)$ up to time $t = 10$, for the Monte Carlo simulation with sample lengths $10,000$ (upper panels) and $50,000$ (lower panels). The mean error (solid line) and 95% confidence intervals (dashed lines) are depicted. Logarithmic scale is used. This figure corresponds to Example 5.1.

Let us compare the performance of different integrators with respect to the first integral $\tilde{H}$ in (4.7). The relative error (5.2) is used as a measure. Fix the polynomial degree 1, for which there are $K = 3$ terms in the expansion, and the system for the coefficients has size 6, with components Q_{1k} and P_{1k}, $k = 1, 2, 3$. In Figure 16, the relative errors are shown. The constant value of the first integral is $\tilde{H}(X(0)) = 2625/37468$. It is clearly appreciated that there is a significant difference between geometric and non-geometric integrators. The errors produced by non-geometric integrators increase with time, whereas geometric integrators present an oscillating, bounded and lower error. The difference is more accentuated than in Figure 6, because of the higher nonlinearity and therefore the higher propagation of error.

Example 5.4. In this example, nonlinearities of non-polynomial type are treated by means of the simple gravity pendulum:

$$\ddot{q} + \omega^2 \sin q = 0, \quad q(0) = q_0, \quad \dot{q}(0) = 0.$$

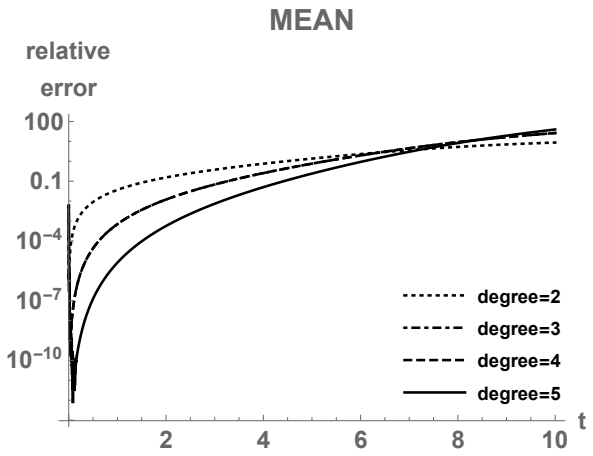

FIGURE 8. Relative errors in the approximation of the mean of $q(t)$ up to time $t = 10$, for finite-term Taylor expansions. Logarithmic scale is used. This figure corresponds to Example 5.1.

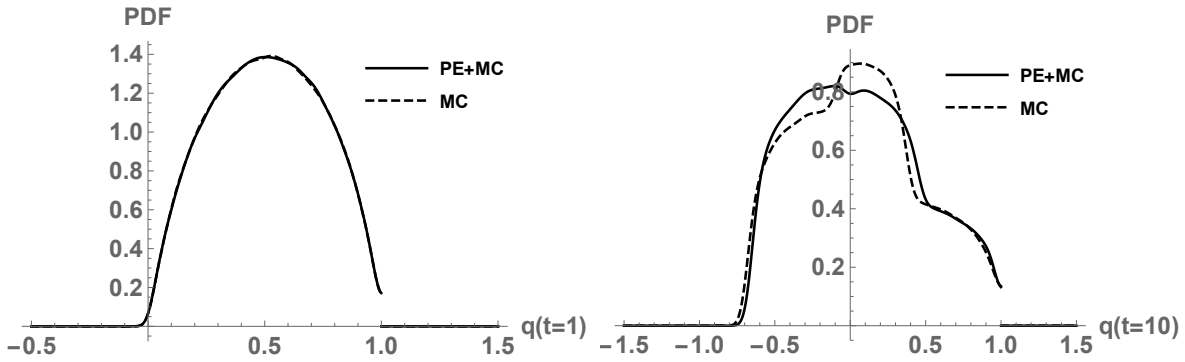

FIGURE 9. Kernel density estimation of the polynomial representation of degree 5 (PE+MC, polynomial expansion plus Monte Carlo) and of $q(t)$ directly (MC, Monte Carlo), at instants $t = 1$ (first panel) and $t = 10$ (second panel). PDF is the probability density function. This figure corresponds to Example 5.1.

The parameter ω^2 is the acceleration of gravity divided by the length of the massless cord. The Hamiltonian reads $H(q,p) = p^2/2 + \omega^2(1 - \cos q)$. It is assumed that $\lambda = (\omega, q_0)$ is a random vector, whose distribution is Dirichlet of parameters $(6, 6, 6)$. Its probability density is

$$f_{(\omega,q_0)}(\omega, q_0) = 205837632\,\omega^5(1 - \omega - q_0)^5, \quad \omega, q_0 > 0, \quad 1 - \omega - q_0 > 0.$$

In the previous examples, the inner products between the vector field of (2.1) and the basis for the construction of the system (4.3)–(4.4) were calculated symbolically, due to the polynomial form of the Hamiltonian H. In the present situation, due to the sine function presence, the determination of the inner products is not straightforward and the construction of the system (4.3)–(4.4) requires quadratures. This issue was fully exposed in the preceding section. It has been checked that, on the square $[0, 1] \times [0, 1]$ with quadrature degree 40, the

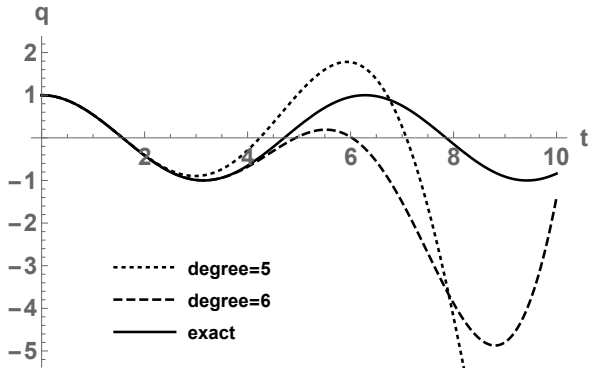

FIGURE 10. For realizations $\omega = 1$ and $q_0 = 1$, polynomial approximations of $q(t) = \cos t$ for times $t \in [0, 10]$. This figure corresponds to Example 5.1.

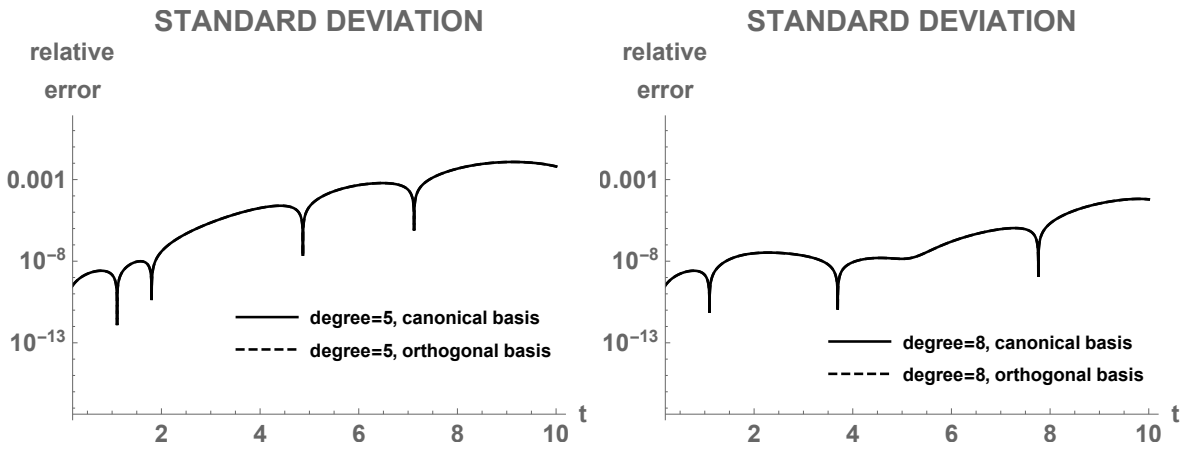

FIGURE 11. Relative errors in the approximation of the standard deviation of $q(t)$, up to time $t = 10$. Expansions with respect to the canonical basis and the orthogonal basis (i.e. gPC) are used (these overlap). The deterministic system of the expansion coefficients is solved by the Störmer-Verlet integrator, with step-size $\Delta t = 0.001$. Logarithmic scale is used. This figure corresponds to Example 5.2.

Gauss-Legendre quadrature gives $\int_{\mathbb{R}^2} f_{(\omega,q_0)}(\omega, q_0)\mathrm{d}\omega\mathrm{d}q_0 = 1$ with an accuracy of 10^{-7}. So, that quadrature degree is used for the inner products.

After this remark, we proceed as the preceding example. First, in Figure 17, the variability of the stochastic problem is showcased by plotting several trajectories in phase space. Times in $[0, 10]$ are considered.

In Figure 18, the mean (the average of Figure 17) and the standard deviation (the dispersion of Figure 17) of the positions and momenta are shown, until time 10. Different degrees are reported. The pictures show that degrees 3 and 4 match. It is perceived that the mean is approximated better than the standard deviation. This is due to the fact that the standard deviation comes from a higher-order moment.

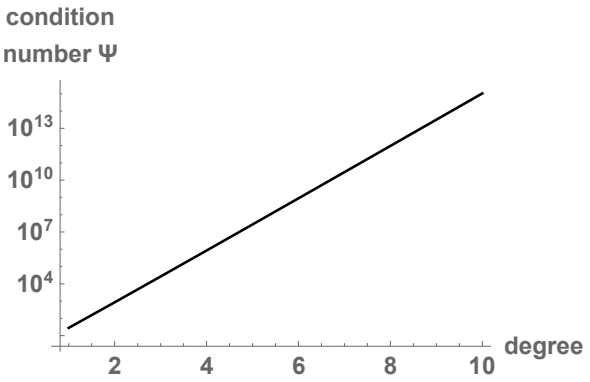

FIGURE 12. Condition number of the Gram matrix Ψ with respect to the polynomial degree of the canonical basis. Logarithmic scale is used. This figure corresponds to Example 5.2.

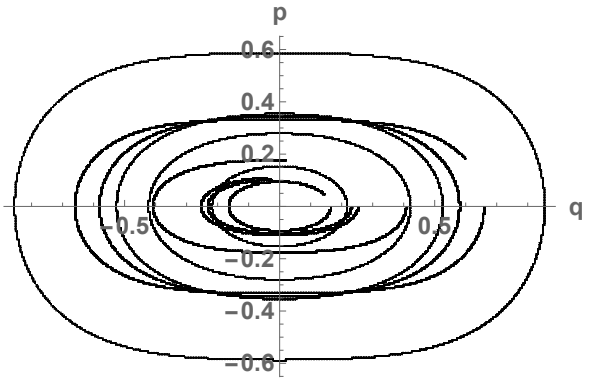

FIGURE 13. Some trajectories of the undamped and unforced Duffing oscillator in phase space, for times $t \in [0, 10]$. The realizations of (α, q_0) have been generated randomly. This figure corresponds to Example 5.3.

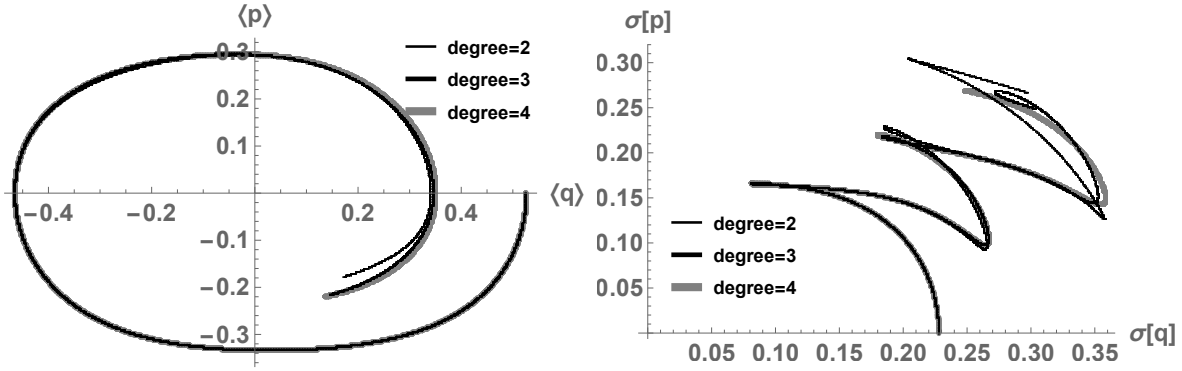

FIGURE 14. Expectation and standard deviation of the positions and momenta, until time $t = 10$. Different degrees are reported. This figure corresponds to Example 5.3.

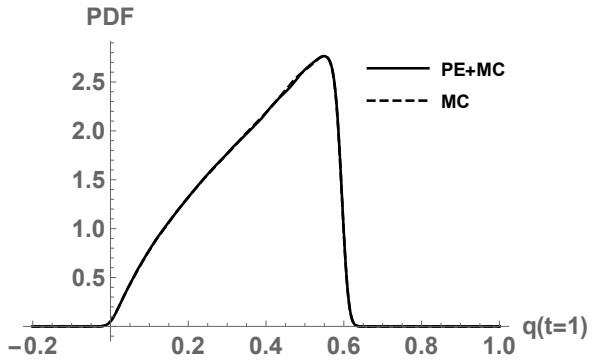

FIGURE 15. Kernel density estimation of the polynomial representation of degree 4 (PE+MC, polynomial expansion plus Monte Carlo) and of the numeric solution $q(t)$ directly (MC, Monte Carlo), at instant $t = 1$. PDF is the probability density function. This figure corresponds to Example 5.3.

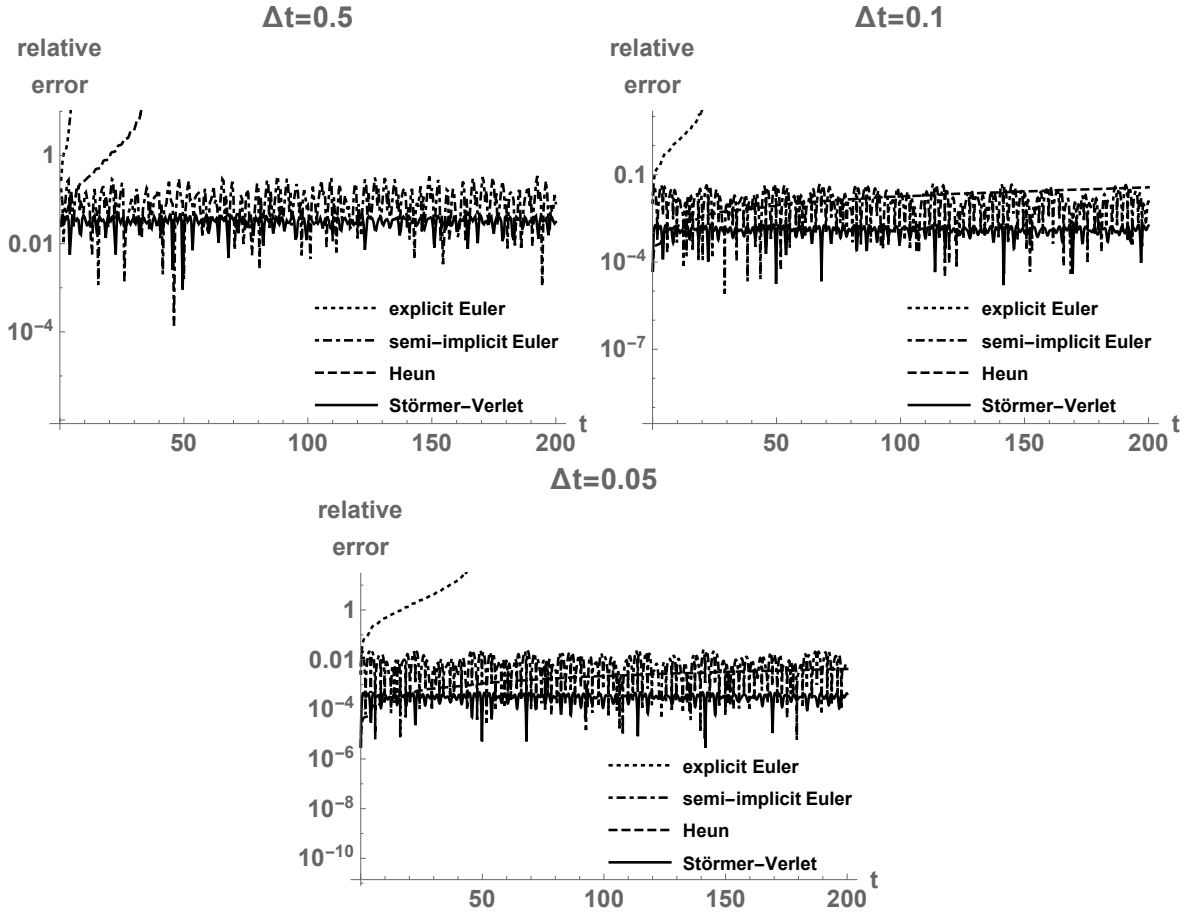

FIGURE 16. Relative errors in $\tilde{H}(X(t))$, where $\tilde{H}$ is the average of H and a first integral, and X is the flow of the system for the coefficients. Times $t \in [0, 200]$ are considered. The polynomial degree 1 is fixed, so that the system has size 6. Different step-sizes Δt are set, as indicated. Logarithmic scale is used. This figure corresponds to Example 5.3.

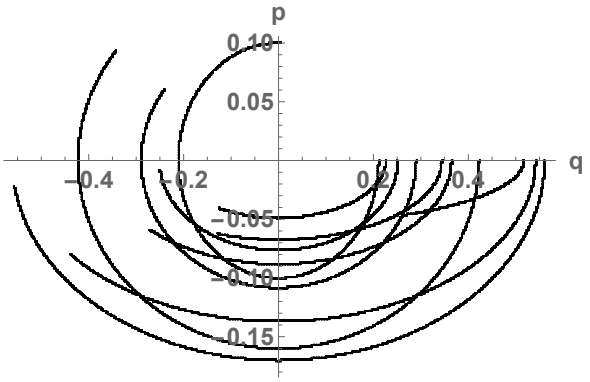

FIGURE 17. Some trajectories of the simple gravity pendulum in phase space, for times $t \in [0, 10]$. The realizations of (ω, q_0) have been generated randomly. This figure corresponds to Example 5.4.

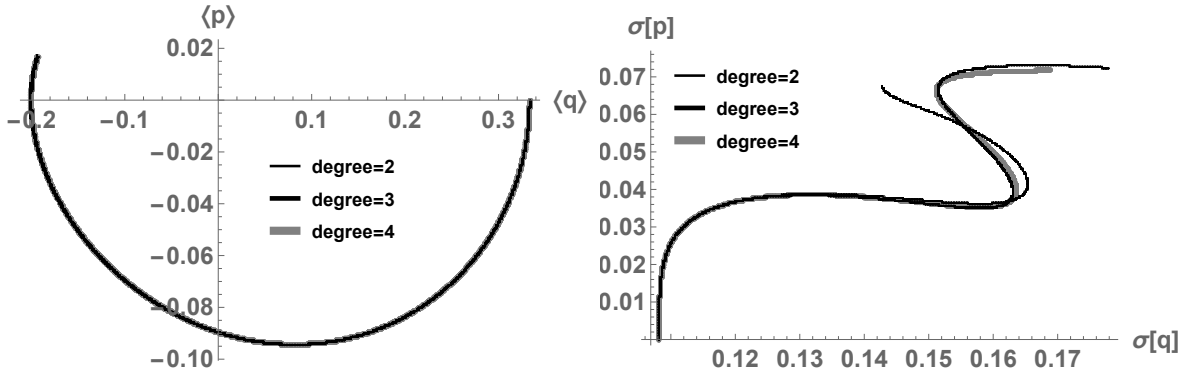

FIGURE 18. Mean and standard deviation of the positions and momenta, until time $t = 10$. Different degrees are reported. This figure corresponds to Example 5.4.

Density approximations are analyzed in Figure 19. For polynomial degree 4, the density estimate is very accurate at $t = 1$, but for $t = 10$ it deviates. Thus, the convergence of densities is poorer than the convergence of mean values.

Different integrators are compared in Figure 20 with respect to the first integral $\tilde{H}$ in (4.7) and the relative error (5.2). The constant value of the first integral is $\tilde{H}(X(0)) = 0.00606798$. This figure is analogous to Figures 6 and 16: the polynomial degree is fixed as 1 and the system for the coefficients has size 6. The pattern of the errors is similar to those past figures.

Example 5.5. All of the previous examples considered input probability distributions for which the moment problem is uniquely solvable. Indeed, their support was bounded. According to the theory of polynomial expansions, this condition is necessary to ensure mean-square convergence. In this example, the purpose is to study a probability distribution for which not all moments exist. Thereby, polynomial representations of high order do not even make sense, because they do not contain statistical information (the mean, the standard deviation, etc. are not well-defined). However, polynomial representations of low or even moderate degree may have well-defined statistics, and they may be used as asymptotic expansions [49]

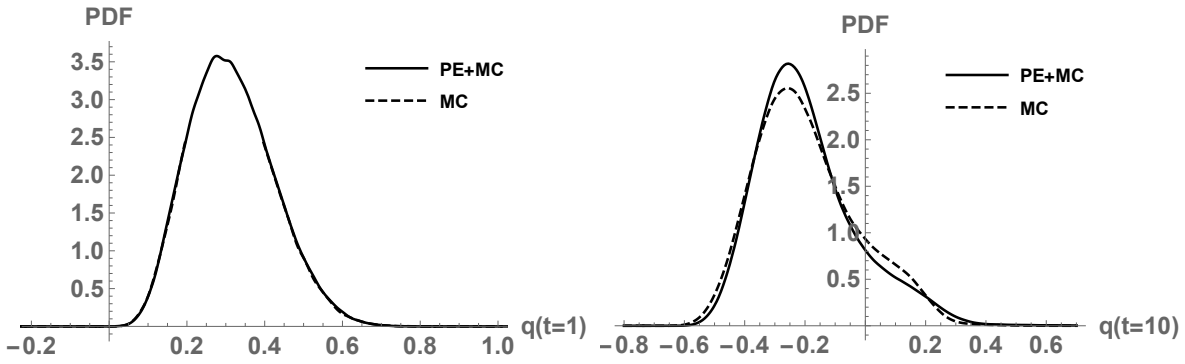

FIGURE 19. Kernel density estimation of the polynomial representation of degree 4 (PE+MC, polynomial expansion plus Monte Carlo) and of the numeric solution $q(t)$ directly (MC, Monte Carlo), at instants $t = 1$ (first panel) and $t = 10$ (second panel). PDF is the probability density function. This figure corresponds to Example 5.4.

to derive accurate approximations of statistics, at least for relatively small time variable. There may be an optimal finite polynomial degree that yields the least error, beyond which the error diverges or the statistic is not well-defined.

Consider the simple gravity pendulum from Example 5.4. It is assumed that $\lambda = (\omega, q_0)$ is distributed as a multivariate Student t distribution with location 0, scale matrix

$$\begin{pmatrix} 0.4 & 0.2 \\ 0.2 & 0.4 \end{pmatrix}$$

and 12 degrees of freedom. Its probability density is

$$f_{(\omega,q_0)}(\omega, q_0) = \frac{5}{2\sqrt{3}\,\pi \left(\frac{1}{12}\left(q_0\left(\frac{10q_0}{3} - \frac{5\omega}{3}\right) + \omega\left(\frac{10\omega}{3} - \frac{5q_0}{3}\right)\right) + 1\right)^7}, \quad \omega, q_0 \in \mathbb{R}.$$

It is a standard result that the Student t distribution does not possess moments of all orders. The larger the number of degrees of freedom is, the larger the number of finite moments is. Therefore, polynomial representations in mean-square evaluated at λ cannot have infinitely many terms.

As in Example 5.4, the construction of the system (4.3)–(4.4) is based on quadratures for the inner products. It has been verified that, on the square $[-7, 7] \times [-7, 7]$ with quadrature degree 60, the Gauss-Legendre quadrature estimates $\int_{\mathbb{R}^2} f_{(\omega,q_0)}(\omega, q_0)\mathrm{d}\omega\mathrm{d}q_0 = 1$ with an accuracy of 10^{-7}. So, that interval and that quadrature degree are selected for the inner products.

In Figure 21, several trajectories in phase space are plotted, for times in $[0, 10]$.

In Figure 22, density approximations are examined for polynomial degree 4. At $t = 0.25$, the approximation is very accurate. But at $t = 1$, errors are clearly visible.

6. Conclusion

Polynomial expansions seem to be a promising tool for uncertainty quantification, as an alternative to statistical methods. For independent input random parameters, gPC expansions and the Galerkin projection technique are of use in the literature. For non-independent

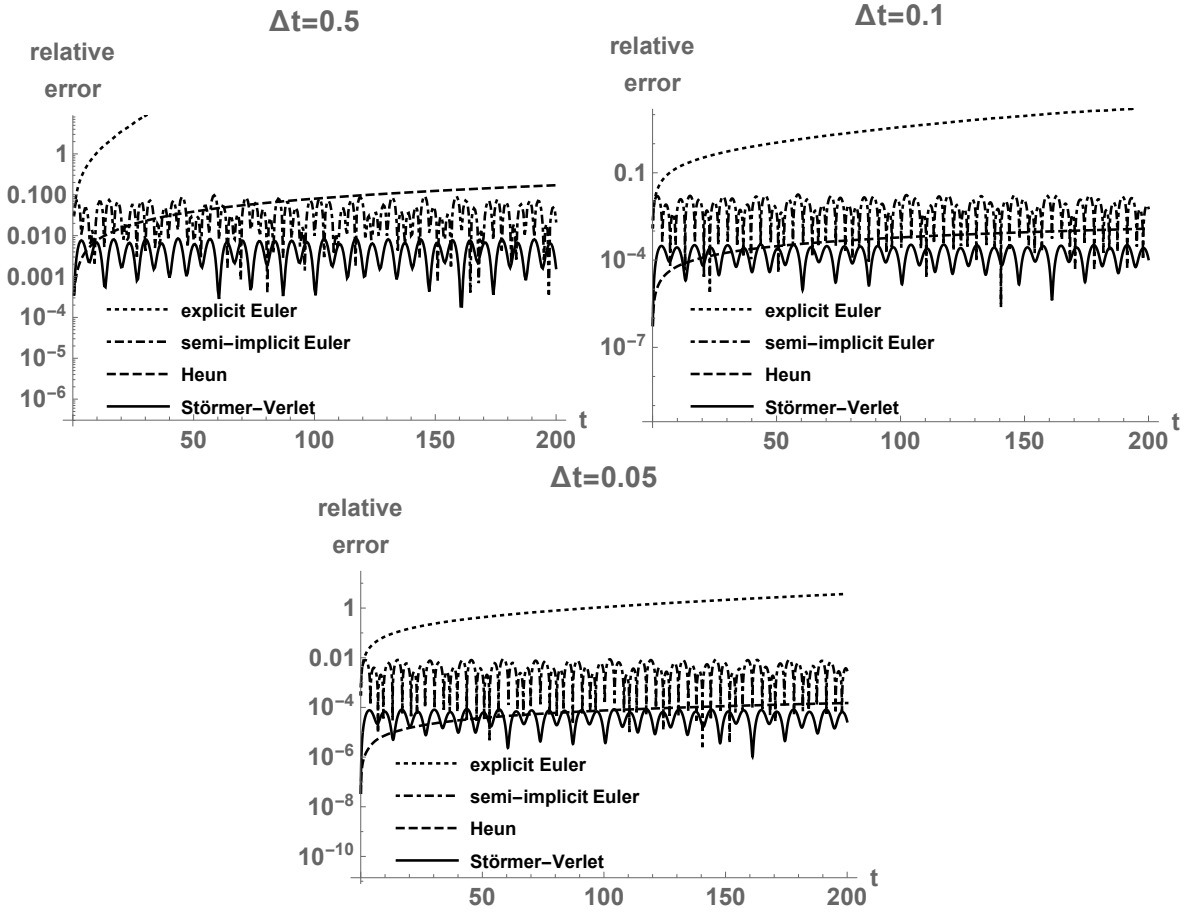

FIGURE 20. Relative errors in $\tilde{H}(X(t))$, where $\tilde{H}$ is the average of H and a first integral, and X is the flow of the system for the coefficients. Times $t \in [0, 200]$ are considered. The polynomial degree 1 is fixed, so that the system has size 6. Different step-sizes Δt are set, as indicated. Logarithmic scale is used. This figure corresponds to Example 5.4.

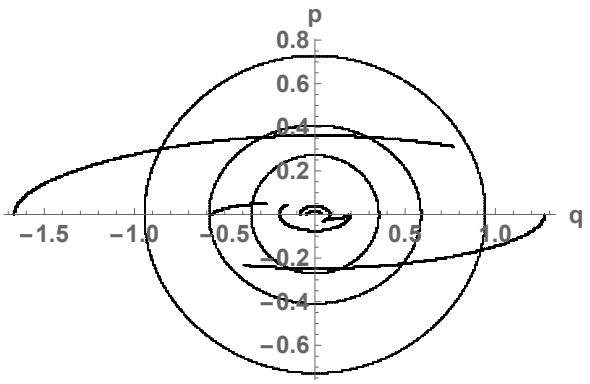

FIGURE 21. Some trajectories of the simple gravity pendulum in phase space, for times $t \in [0, 10]$. The realizations of (ω, q_0) have been generated randomly. This figure corresponds to Example 5.5.

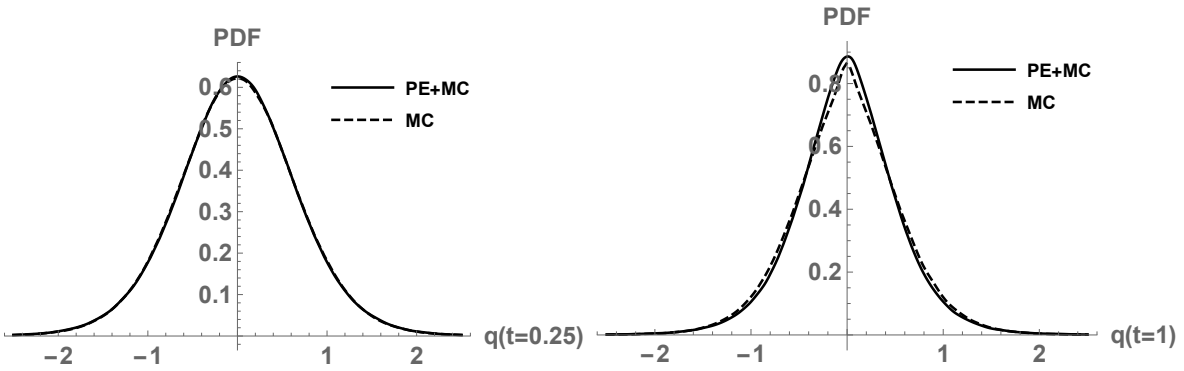

FIGURE 22. Kernel density estimation of the polynomial representation of degree 4 (PE+MC, polynomial expansion plus Monte Carlo) and of the numeric solution $q(t)$ directly (MC, Monte Carlo), at instants $t = 0.25$ (first panel) and $t = 1$ (second panel). PDF is the probability density function. This figure corresponds to Example 5.5.

inputs and with the motivation of extending the gPC theory, polynomial expansions in terms of the canonical polynomial basis and an imitation of the Galerkin projection technique are employed. In such a case, no Gram-Schmidt orthogonalization procedure is necessary, but the Gram matrix is not the identity and may be highly ill-conditioned. In all cases, the polynomial coefficients are obtained by solving a deterministic system, which is larger than the original model. If this deterministic system can be solved efficiently, then a single integration already gives a faithful polynomial representation of the model solution. This entails an improvement over Monte Carlo simulation, which demands a vast number of integrations of the governing model. Once the polynomial representation is realized, the post-treatment stage starts: statistical characteristics are extracted analytically (mean and variance) or by sampling (density, percentiles, probabilities, etc.).

For random Hamiltonian systems with independent inputs, the gPC-based Galerkin approach gives rise to a Hamiltonian Galerkin system for the coefficients. Its Hamiltonian is the average of the initial Hamiltonian. For non-independent inputs, the approach investigated in the present paper gives rise to a volume-preserving, reversible (if even with respect to momenta), non-Hamiltonian system, with a first integral given by the average of the initial Hamiltonian. Because of the special structure of this system, the classical symplectic integrators from Hamiltonian dynamics are volume preserving. Not all volume-preserving systems satisfy this notable property.

The numerical examples, based on prototypical Hamiltonian models with uncertainties and the Störmer-Verlet integrator, reveal the applicability of the method. This integrator is volume preserving, symmetric and reversible, and the error for the first integral is oscillating, bounded and low. Classical non-geometric integrators, by contrast, present an error growth in time for the first integral. Further investigation for the future shall be devoted to Poisson integrators [23].

As occurs with gPC, the method is limited to smooth dynamics, low random dimensionality and moderate time variable, as opposed to Monte Carlo simulation. Optimality is obtained for mean-square convergence, even though we cannot get rid of the global Lipschitz condition in the theoretical development. Numerically, it is evinced that the rates of convergence

for densities and for pointwise realizations are poorer. These issues demand more rigorous mathematical analysis.

In general, the theory behind the polynomial representations requires that the moment problem for the input random parameters is uniquely solvable. However, even for input distributions for which not all moments exist (such as the Student t distribution), it might be possible to employ polynomial representations under the notion of asymptotic expansion, at least for relatively small time variable. Polynomial representations of low or even moderate degree may have well-defined statistics. There may be an optimal finite polynomial degree that yields the least error, beyond which the error diverges or the statistic is not well-defined. This is shown in the last numerical example.

This work is devoted to forward uncertainty quantification. Inverse uncertainty quantification is usually carried out by relying on Bayesian inference. Though not treated in this work, let us mention that the likelihood of the Bayesian model may be approximated by polynomials, so that each step of the Markov Chain Monte Carlo algorithm simply requires polynomial evaluations. The polynomials are constructed from the prior distributions of the parameters. If these are independent, then gPC and Galerkin projections are of use [50–52]. But maybe complex prior information leads to non-independent prior distributions. In such a case, the polynomial expansions investigated in this paper are applicable (of course, as long as the random dimensionality is low).

Other topics of interest, for which gPC has shown fruitful applications, are random geometries in the specification of the physical domain [53] and the ensemble Kalman filter [54]. For non-independent inputs, maybe one could take advantage of the polynomial expansions investigated in the present paper.

Funding

Marc Jornet has been supported by a postdoctoral contract from Universitat Jaume I, Spain (Acció 3.2 del Pla de Promoció de la Investigació de la Universitat Jaume I per a l'any 2020). He has also been funded by project UJI-B2019-17 from Universitat Jaume I, Spain.

Conflict of Interest Statement

The author declares that there is no conflict of interests regarding the publication of this article.

References

[1] A. Iserles. A First Course in the Numerical Analysis of Differential Equations. Cambridge University Press, 2009.
[2] R.J. LeVeque. Finite Difference Methods for Ordinary and Partial Differential Equations: Steady-State and Time-Dependent Problems. SIAM, 2007.
[3] R.E. Mickens (Ed.). Advances on Applications of Nonstandard Finite Difference Schemes. World Scientific, Singapore, 2005.
[4] S. Blanes, F. Casas. A Concise Introduction to Geometric Numerical Integration. CRC Press, 2017.
[5] D. Xiu. Numerical Methods for Stochastic Computations: A Spectral Method Approach. Cambridge Texts in Applied Mathematics. Princeton University Press, 2010.
[6] O.P. Le Maître, O.M. Knio. Spectral Methods for Uncertainty Quantification: With Applications to Computational Fluid Dynamics. Springer Science & Business Media, Netherlands, 2010.
[7] R.C. Smith. Uncertainty Quantification: Theory, Implementation, and Applications. SIAM, 2013.

[8] G. Fishman. Monte Carlo: Concepts, Algorithms, and Applications. Springer Science & Business Media, Springer Series in Operations Research and Financial Engineering, New York, 1996.
[9] R.E. Caflisch. Monte Carlo and quasi-Monte Carlo methods. Acta Numerica, 7 (1998): 1–49.
[10] D. Xiu, G.E. Karniadakis. The Wiener–Askey polynomial chaos for stochastic differential equations. SIAM Journal on Scientific Computing, 24(2) (2002): 619–644.
[11] R. Ghanem, P. Spanos. Stochastic Finite Elements: A Spectral Approach. Springer-Verlag, New York, 1991.
[12] O.G. Ernst, A. Mugler, H.J. Starkloff, E. Ullmann. On the convergence of generalized polynomial chaos expansions. ESAIM: Mathematical Modelling and Numerical Analysis, 46(2) (2012): 317–339.
[13] M. Gerritsma, J.B. Van der Steen, P. Vos, G. Karniadakis. Time-dependent generalized polynomial chaos. Journal of Computational Physics, 229(22) (2010): 8333–8363.
[14] D. Gottlieb, D. Xiu. Galerkin method for wave equations with uncertain coefficients. Communications in Computational Physics, 3(2) (2008): 505–518.
[15] D. Xiu. Efficient collocational approach for parametric uncertainty analysis. Communications in Computational Physics, 2(2) (2007): 293–309.
[16] D. Xiu. Fast numerical methods for stochastic computations: a review. Communications in Computational Physics, 5(2–4) (2009): 242–272.
[17] J.M. Pasini, T. Sahai. Polynomial chaos based uncertainty quantification in Hamiltonian, multi-time scale, and chaotic systems. Journal of Computational Dynamics, 1(2) (2014): 357–375.
[18] N. Bou-Rabee, J.M. Sanz-Serna. Geometric integrators and the Hamiltonian Monte Carlo method. Acta Numerica (2018): 113–206.
[19] J.C. Cortés, J.V. Romero, M.D. Roselló, F.J. Santonja, R.J. Villanueva. Solving continuous models with dependent uncertainty: a computational approach. Abstract and Applied Analysis, 2013(ID 983839) (2013): 10.
[20] J. Calatayud, J.C. Cortés, M. Jornet. Uncertainty quantification for nonlinear difference equations with dependent random inputs via a stochastic Galerkin projection technique. Communications in Nonlinear Science and Numerical Simulation, 72 (2019): 108–120.
[21] J. Calatayud, J.C. Cortés, M. Jornet, L. Villafuerte. Is It Worthwhile Considering Orthogonality in Generalised Polynomial Chaos Expansions Applied to Solving Stochastic Models?. Computational Mathematics and Applications. Springer, Singapore, 2020. Pages 261–277.
[22] B. Adcock, D. Huybrechs. Frames and numerical approximation. SIAM Review, 61(3) (2019): 443–473.
[23] E. Hairer, C. Lubich, G. Wanner. Geometric Numerical Integration. Volume 31 of Springer Series in Computational Mathematics. Springer, Heidelberg, 2010.
[24] R. Syski. Stochastic Differential Equations. Modern Nonlinear Equations. Dover, 1967. Pages 346–456.
[25] T. Neckel, F. Rupp. Random Differential Equations in Scientific Computing. Walter de Gruyter, 2013.
[26] X. Mao. Stochastic Differential Equations and Applications. Second edition, Elsevier, 2007.
[27] E. Allen. Modeling With Itô Stochastic Differential Equations. Dordrecht, Netherlands: Springer Science & Business Media, 2007.
[28] H.T. Banks, J.L. Davis, S.L. Ernstberger, S. Hu, E. Artimovich, A.K. Dhar, C.L. Browdy. A comparison of probabilistic and stochastic formulations in modelling growth uncertainty and variability. Journal of Biological Dynamics, 3(2–3) (2009): 130–148.
[29] J.A.S. Witteveen, H. Bijl. Modeling arbitrary uncertainties using Gram-Schmidt polynomial chaos. Proceedings of the 44th AIAA Aerospace Sciences Meeting and Exhibit, AIAA-2006-0896, Reno, Nevada, 9–12 January 2006.
[30] R.H. Cameron, W.T. Martin. The orthogonal development of non-linear functionals in series of Fourier-Hermite functionals. The Annals of Mathematics, 48(2) (1947): 385–392.
[31] R.V. Field Jr, M.D. Grigoriu. Convergence properties of polynomial chaos approximations for L_2 random variables. SAND2007-1262, Sandia National Laboratories, 2007.
[32] R. Courant, D. Hilbert. Methods of Mathematical Physics. John Wiley & Sons, New York, 1953.
[33] D. Funaro. Polynomial Approximation of Differential Equations. Springer-Verlag, Berlin, 1992.
[34] W. Shi, C. Zhang. Error analysis of generalized polynomial chaos for nonlinear random ordinary differential equations. Applied Numerical Mathematics, 62(12) (2012): 1954–1964.

[35] J.L. Strand. Random ordinary differential equations. Journal of Differential Equations, 7(3) (1970): 538–553.
[36] M. Rosenblatt. Remarks on a multivariate transformation. Annals of Mathematical Statistics, 23(3) (1953): 470–472.
[37] J.D. Jakeman, F. Franzelin, A. Narayan, M.S. Eldred, D. Plfüger. Polynomial chaos expansions for dependent random variables. Computer Methods in Applied Mechanics and Engineering, 351 (2019): 643–666.
[38] T.T. Soong. Random Differential Equations in Science and Engineering. Academic Press, New York, 1973.
[39] W.K. Liu, T. Belytschko, A. Mani. Probabilistic finite elements for nonlinear structural dynamics. Computer Methods in Applied Mechanics and Engineering, 56(1) (1986): 61–81.
[40] W.K. Liu, T. Belytschko, A. Mani. Random field finite elements. International Journal for Numerical Methods in Engineering, 23(10) (1986): 1831–1845.
[41] M. Kamiński, G.F. Carey. Stochastic perturbation-based finite element approach to fluid flow problems. International Journal of Numerical Methods for Heat & Fluid Flow, 15(7) (2005): 671–697.
[42] M. Jornet. On the applicability of the perturbation method for the random viscous Burgers' equation. Indian Journal of Physics, (2021): 1–3. Doi: 10.1007/s12648-020-01897-y.
[43] D. Hilbert. Ein beitrag zur theorie des legendre'schen polynoms. Acta Mathematica, 18(1) (1894): 155–159.
[44] M.D. Choi. Tricks or treats with the Hilbert matrix. The American Mathematical Monthly, 90(5) (1983): 301–312.
[45] J. Todd. The condition of the finite segments of the Hilbert matrix. In: Contributions to the solution of systems of linear equations and the determination of eigenvalues, 39. National Bureau of Standards Applied Mathematics Series, 1954. Pages 109–116.
[46] O. Taussky. A remark concerning the characteristic roots of the finite segments of the Hilbert matrix. The Quarterly Journal of Mathematics, 1 (1949): 80–83.
[47] P. Otte. Upper bounds for the spectral radius of the $n \times n$ Hilbert matrix. Pacific Journal of Mathematics, 219(2) (2005):323–331.
[48] K. Feng, Z. Shang. Volume-preserving algorithms for source-free dynamical systems. Numerische Mathematik, 71(4) (1995): 451–463.
[49] A.H. Nayfeh. Perturbation Methods. John Wiley & Sons, Germany, 2008.
[50] Y.M. Marzouk, H.N. Najm, L.A. Rahn. Stochastic spectral methods for efficient Bayesian solution of inverse problems. Journal of Computational Physics, 224(2) (2007): 560–586.
[51] Y. Marzouk, D. Xiu. A stochastic collocation approach to Bayesian inference in inverse problems. Communications in Computational Physics, 6(4) (2009): 826–847.
[52] J.B. Nagel, B. Sudret. Spectral likelihood expansions for Bayesian inference. Journal of Computational Physics, 309 (2016): 267–294.
[53] D. Xiu, D.M. Tartakovsky. Numerical methods for differential equations in random domains. SIAM Journal on Scientific Computing, 28(3) (2006): 1167–1185.
[54] J. Li, D. Xiu. A generalized polynomial chaos based ensemble Kalman filter with high accuracy. Journal of Computational Physics, 228 (2009): 5454–5469.